Research Paper

The lipidomes of *C. elegans* with mutations in *asm-3*/acid sphingomyelinase and *hyl-2*/ceramide synthase show distinct lipid profiles during aging

Trisha A. Staab[1], Grace McIntyre[1], Lu Wang[2], Joycelyn Radeny[4], Lisa Bettcher[3], Melissa Guillen[1], Margaret P. Peck[4], Azia P. Kalil[4], Samantha P. Bromley[4], Daniel Raftery[3], Jason P. Chan[1]

[1]Department of Biology, Marian University, Indianapolis, IN 46222, USA
[2]Department of Environmental and Occupational Health Sciences, University of Washington, Seattle, WA 98195, USA
[3]Northwest Metabolomics Research Center, University of Washington, Seattle, WA 98195, USA
[4]Department of Biology, Juniata College, Huntingdon, PA 16652, USA

Correspondence to: Jason P. Chan; **email:** jpchan@me.com, https://orcid.org/0000-0001-8123-536X

ABSTRACT

Lipid metabolism affects cell and physiological functions that mediate animal healthspan and lifespan. Lipidomics approaches in model organisms have allowed us to better understand changes in lipid composition related to age and lifespan. Here, using the model *C. elegans*, we examine the lipidomes of mutants lacking enzymes critical for sphingolipid metabolism; specifically, we examine acid sphingomyelinase (*asm-3*), which breaks down sphingomyelin to ceramide, and ceramide synthase (*hyl-2*), which synthesizes ceramide from sphingosine. Worm *asm-3* and *hyl-2* mutants have been previously found to be long- and short-lived, respectively. We analyzed longitudinal lipid changes in wild type animals compared to mutants at 1-, 5-, and 10-days of age. We detected over 700 different lipids in several lipid classes. Results indicate that wildtype animals exhibit increased triacylglycerols (TAG) at 10-days compared to 1-day, and decreased lysophoshatidylcholines (LPC). We find that 10-day *hyl-2* mutants have elevated total polyunsaturated fatty acids (PUFA) and increased LPCs compared to 10-day wildtype animals. These changes mirror another short-lived model, the *daf-16*/FOXO transcription factor that is downstream of the insulin-like signaling pathway. In addition, we find that *hyl-2* mutants have poor oxidative stress response, supporting a model where mutants with elevated PUFAs may accumulate more oxidative damage. On the other hand, 10-day *asm-3* mutants have fewer TAGs. Intriguingly, *asm-3* mutants have a similar lipid composition as the long-lived, caloric restriction model *eat-2*/mAChR mutant. Together, these analyses highlight the utility of lipidomic analyses to characterize metabolic changes during aging in *C. elegans*.

INTRODUCTION

Lipidomic analysis is an emerging field for investigating lifespan regulation and age-related diseases. Lipidomic profiles can be determinants of lifespan and disease conditions [1, 2]. For example, lipid classes including fatty acids (FA), triacylglycerols (TAG), sphingolipids (SL), and phospholipids (PL) have been identified as targets in lipid signatures related to aging [2, 3]. Furthermore, specific signatures are detected in the lipid profiles of those with age-related diseases, such as Alzheimer's Disease [4–9]. In addition, the abundance

of many fatty acid subtypes differs between the youth, elderly, and centenarians [10, 11].

Lipids serve diverse functions and occur in varied locations within cells. The lipid composition of cell membranes can affect aging processes through regulating protein localization, peroxidation, and cell structure. Intracellular lipids, on the other hand, can be involved in signaling, be sources of energy storage, and affect trafficking and organelle functions related to stress responses [12, 13]. For example, the degree of saturation of membrane fatty acids and the levels of polyunsaturated fatty acids (PUFAs) may mediate oxidative damage associated with aging cells [2]. Lipid analyses using model organisms have correlated longevity to elevated PUFAs, as these long carbon chains are more susceptible to oxidative damage [2, 14]. Furthermore, breakdown of lipid droplets that store TAG through lipophagy may release specific fatty acids that mediate the transcriptional regulation of genes involved in stress response and longevity [13, 15, 16]. While TAG levels determine cellular energy storage, total TAGs may have both beneficial and detrimental roles depending on the type of lipid and the organism [17, 18].

Sphingolipid changes are observed in lipidomic profiles associated with age, making it an interesting biomarker for aging [19]; in particular, sphingomyelin (SM) abundance is associated with lifespan in several organisms, including *C. elegans* [20–23]. For example, mutants lacking acid sphingomyelinase (*asm-3*) have longer lifespans [24]. Interestingly, ASM-3 may interact with the DAF-2/insulin-like growth factor receptor, possibly by regulating receptor localization, as loss of *asm-3* increased the nuclear localization of the DAF-16/FOXO transcription factor that is normally inhibited by DAF-2 [24, 25]. Indeed, further evidence supports that sphingolipids make up a major component of microdomains in cell membranes and may mediate protein localization, including receptor localization [26–28]. Interestingly, specific sphingolipid metabolism enzymes, including sphingomyelinase and ceramidase, may have increased activity during aging in rats [29]. However, it is not clear how changes in sphingolipid metabolic enzymes may impact other sphingolipids and larger lipidomic changes.

Many of the metabolic enzymes that mediate lipid synthesis or breakdown have been linked to stress response and aging in organisms [1]. For example, several genes involved with fatty acid elongation (*Elovl5*), desaturation (*Scd5*), and mitochondrial fatty acid synthesis (*Mecr* and *Oxsm*) have been identified as targets of natural selection related to increased lifespan in mammals [30]. In *C. elegans*, fatty acid elongation also seems important for aging [1, 31]. For

example, knockdown of *elo-2*, a fatty acid elongase, results in increased lifespan, while knockdown of *elo-5* decreases lifespan. In addition, genetic studies targeting sphingolipid metabolism suggest that specific enzymes may mediate lifespan in worms and flies, and chronological and replicative lifespan in yeast [25, 32–34].

Studies identifying new regulators of aging are critical, given the global rise in an aging population. Lipidomic studies serve as a powerful approach to identify specific metabolic pathways that may contribute to organismal longevity, healthy aging, or pathology. Indeed, lipidomic approaches in long-lived humans and model organisms have provided insight into the lipid changes associated with healthy aging [1, 17, 35]. In particular, work using *C. elegans* have identified age related changes in specific lipids, lipid classes, as well as the ratio of monosaturated to polysaturated fatty acids (MUFA:PUFA ratio) [36, 37]. Here, we examine the lipidomes of animals lacking the sphingolipid metabolism enzymes, *asm-3*/acid sphingomyelinase or *hyl-2*/ceramide synthase, which have previously been shown to have extended and reduced lifespans, respectively, in *C. elegans* [24, 34, 38]. Understanding enzymatic regulation of sphingolipid metabolism is valuable, as changes to sphingomyelins and ceramides impact cell membranes, cell death signaling, and aging [39]. Using *asm-3* and *hyl-2* mutants, we find that each has a unique lipidome compared to wild type, and each shares a similar lipid profile with other short and long-lived *C. elegans* models of aging, respectively. These findings add to our understanding of lipid changes associated with aging.

RESULTS

Altering ceramide metabolism affects oxidative stress responses and lipid abundance

Previous work has shown that *C. elegans* with abnormal ceramide metabolism have altered lifespans and stress response. For example, genetic manipulations leading to the loss of *hyl-2*/CER synthase - which makes ceramide (Figure 1A) - result in shortened lifespans, hypersensitivity to anoxia, and poor survival to heat stress [34, 38, 40]. On the other hand, genetic and pharmacological manipulations that inhibit *asm-3*/acid sphingomyelinase - which converts sphingomyelin to ceramide - increase lifespan [24, 25]. Here, we explored the age-related response of *hyl-2* and *asm-3* mutants to oxidative stress induced by juglone (JG). We found that *hyl-2* mutants at both young and old ages are more sensitive to oxidative stress compared to wildtype (N2) animals. Specifically, survival of *hyl-2* animals exposed to 150μM juglone decreased significantly from wildtype

animals at 1 and 10 days of age (Kaplan-Meier estimate and log rank test; $p=8.5e-11$ and $p=0.01455$ respectively), while *asm-3* mutants did not differ from wildtype animals at either age ($p>0.05$ for both; Figure 1B). *hyl-2* mutants showed a similar response to paraquat (PQ) (Supplementary Figure 1).

Given the links between lipid profiles and aging, we next tested whether loss of *hyl-2* or *asm-3* altered lipid abundance using Nile red, a stain primarily for neutral lipids such as triglycerides, and may particularly label lysosomal related organelles [41, 42]. We found that 10-day old animals had greater Nile red staining compared to their 1-day counterparts ($p<0.001$ for all genotypes). Comparing across genotypes showed that 10-day *hyl-2* mutants had significantly less Nile red staining than N2 animals ($p=9.8e-4$) but not at the 1-day timepoint

($p=0.61$); contrary, *asm-3* animals were not statistically different from N2 on either day. These findings suggest that manipulations in ceramide metabolism may produce broad lipid changes in older animals.

Lipidomes of *hyl-2* and *asm-3* mutants show differential lipid changes

To explore specific lipid changes in *asm-3* and *hyl-2* mutants, we used a lipidomics approach to evaluate changes in specific lipid molecules and classes of lipids. Using shotgun lipidomics by electrospray ionization (ESI) and mass spectrometry, we sampled six independent replicates of 1-, 5-, and 10-day old adult worms of different genotypes. We profiled N2, *asm-3,* and *hyl-2* animals as well as two well-studied mutant models of aging (the short-lived *daf-16*/FOXO mutant and the
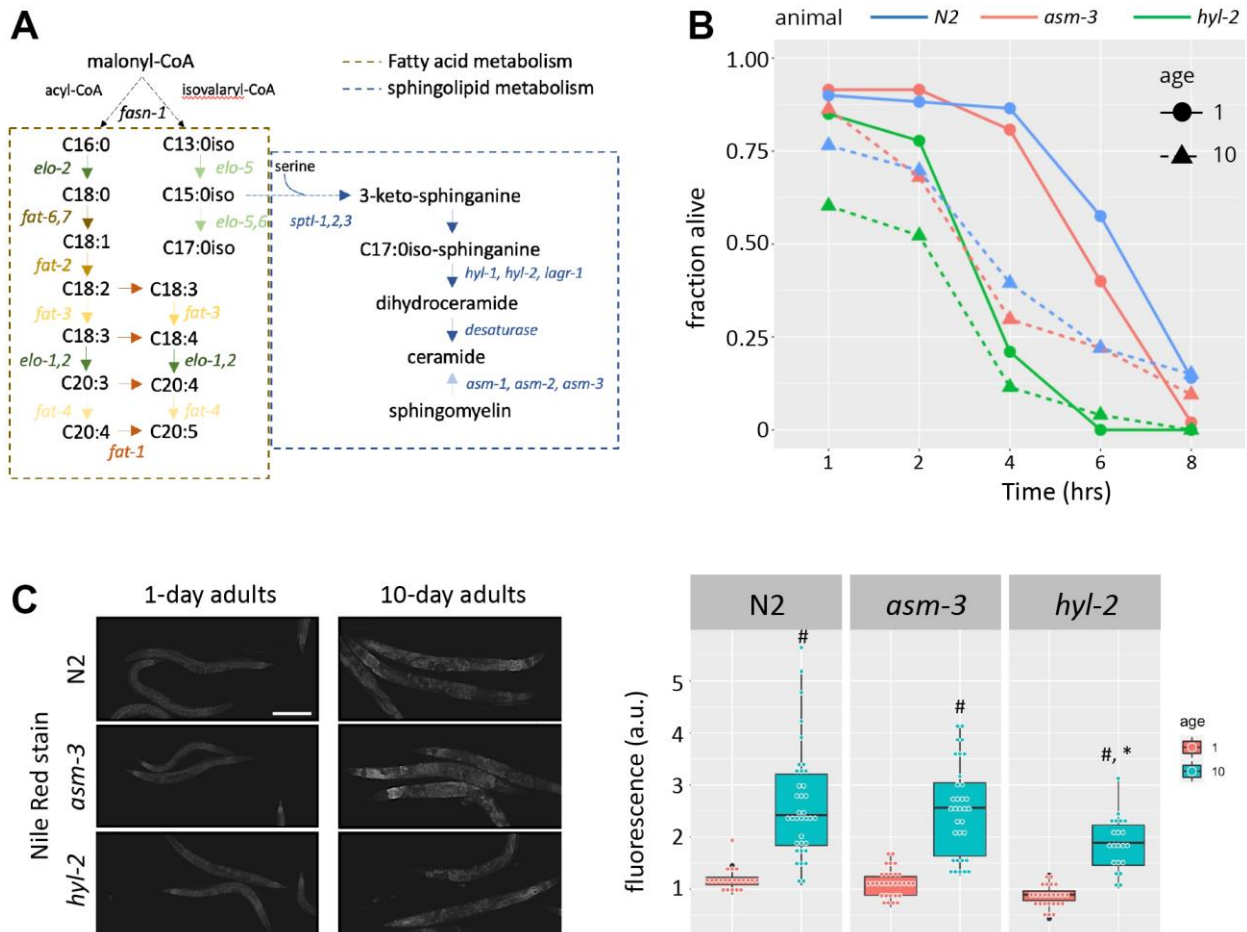
Figure 1. Loss of *hyl-2*/CER synthase results in poor oxidative stress responses. (**A**) Diagram showing the lipid pathways and metabolic enzymes producing free fatty acids (FFAs) and sphingolipids (SLs). (**B**) Survival of 1-, 5-, and 10-day old N2 (blue), *asm-3* (red), and *hyl-2* (green) worms treated with 150μM juglone. Worms were treated with juglone in 96 well plates, and survival was determined by a movement response to agitation. Survival curves were analyzed using Kaplan-Meier estimate and pairwise differences were determined using log-rank tests (n=49 for N2 1 day; n=48 for N2 10 day; n=46 for *asm-3* 1 day; n=35 for *asm-3* 10 day; n=28 for *hyl-2* 1 day; n=44 for *hyl-2* 10 day). (**C**) Representative images (left) and fluorescence quantification (right) of Nile Red lipid staining in 1-day and 10-day old N2, *asm-3*, and *hyl-2* animals. #indicates $p<0.05$ compared to 1-day counterpart of the same genotype and *indicates $p<0.05$ compared to N2 counterpart of the same age.

long-lived, calorically restricted *eat-2*/mAChR mutant). Overall, 701 lipids were identified and analyzed covering phosphatidylcholines (PC), phosphatidylethanolamines (PE), lysophosphatidylcholines (LPC), lysophosphatidylethanolamine (LPE), sphingomyelins (SM), cholesterol esters (CE), ceramides (CER), free fatty acids (FFA), diacylglycerols (DAG), and triacylglycerols (TAG). We detected significant differences in class composition between the different strains and age groups compared to 1-day old N2 adults (Supplementary Figure 2). Interestingly, TAG increased in 10-day old animals compared to 1-day old animals in N2, *daf-16,* and *hyl-2* animals. However, this increase was not observed in long-lived *eat-2* or *asm-3* animals. Overall, we found that our samples had 12.1% FFA, 26.1% TAG, 2.0% DAG, 35.0% PEs, and 16.0% PCs, which is somewhat comparable to that observed in yolk (16.2%, 26.4%, 3.2%, 28.2% and 23%, reference [43]). However, lipid composition is likely to vary by technique and tissue preparation [44].

To visualize how age affects lipidome changes, we first examined how well lipidomes clustered by age or genotype using principal components analysis (PCA). For this analysis, raw concentrations of each lipid were *log₂* transformed and analyzed. We found that within each genotype, animals from each age group clustered most closely with animals from the same age group (Figure 2A–2F). This suggests that age is a major driver of lipid profiles regardless of genotype. Interestingly, when analyzing the PCA plots by age, genotypes appear to cluster more closely at 1-day, except *daf-16* mutants which appear to cluster away from the rest (Figure 2G, 2H). This visual representation suggests that as animals age, their lipid profile may become more distinct by genotype. Thus, we performed more detailed analysis of specific changes.

Next, we determined whether age affected the lipidome within specific classes of lipids. To do this, we visualized lipid concentrations through heatmaps of free fatty acids (FFA) in N2, *asm-3*, and *hyl-2* mutants (Figure 3A). Wildtype N2 animal show decreases in many shorter chained FFAs, particularly saturated FFA. The largest decreases were in FFA(20:0) (log_2FC = -2.6, *FDR*=1.60e-15), FFA(18:0) (log_2FC = -2.5, FDR=2.61e-19) (Supplementary Tables 2, 5). This observation is more pronounced in *asm-3* mutants. However, *hyl-2* mutants show increases in FFA of most types from 1 to 10 days, including many of shorter chained saturated and unsaturated FFAs; this is similar to the short-lived *daf-16* mutant. Interestingly, long-lived *eat-2* and *daf-2* mutants have been shown to have lower amounts of shorter chained fatty acids (C14:0 - C20:0) [6], suggesting that shorter chain FA may contribute to aging. However, very long chain polyunsaturated FFAs increase with age in wildtype animals (Figure 3 and Supplementary Tables 2, 5). The
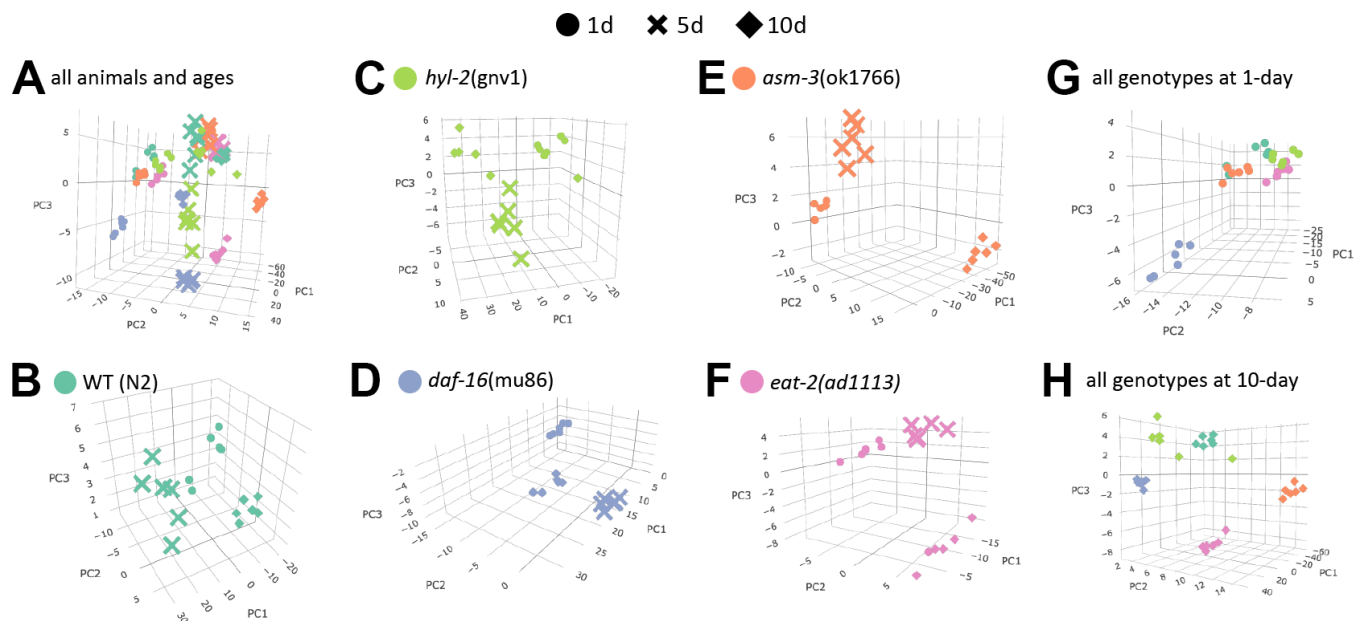
Figure 2. Age is a major determinant of lipid profiles in *C. elegans*. Principal component analysis (PCA) graphs show lipid profiles by 1-day (circles), 5-day (cross bars), and 10-day (diamonds). (**A**) PCA graph showing variation all groups, by strain and age. (**B–F**) PCA graphs showing variations in age by strain (different colors as indicated). (**G–H**) PCA graphs showing variations by 1-day old animals (**G**) and 10-day old animals (**H**).
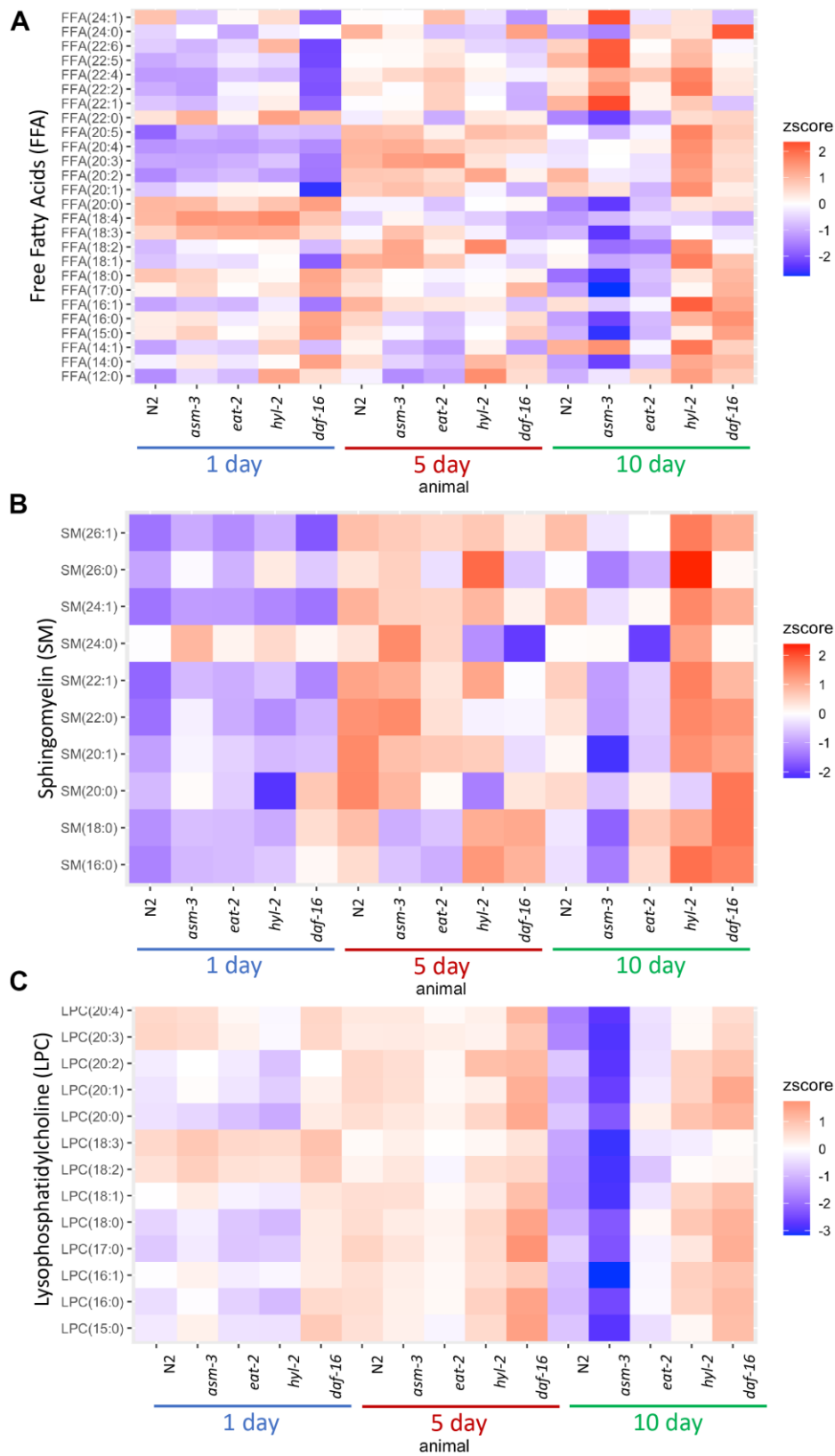
Figure 3. Lipid profiles vary by age and genotype. Heatmaps showing average z-score of log2 concentration for (**A**) free fatty acids (FFA), (**B**) sphingomyelins, and (**C**) lysophosphatidylcholines (LPCs). For sphingomyelins, the lipid ID does not include the 18:1 fatty acid chain, and LIPIDMAPS nomenclature is reported in Supplementary Table 11. Wildtype, *asm-3*, *eat-2, hyl-2,* and *daf-16* worms were analyzed at 1-, 5- and 10-days old. For all, the heatmaps show averaged z scores for the six replicates in each group.

largest changes of FFA from 1 day to 10 day N2 were in polyunsaturated FFA(20:2) ($\log_2$FC = 2.3, FDR=1.99e-34) and FFA(22:5) ($\log_2$FC = 1.30, FDR=1.75e-14). Interestingly, *asm-3* mutants exhibit increases in many of the longer chained FFAs at 10 days compared to 1 day (Figure 3A and Supplementary Tables 3, 8).

We then examined sphingomyelin (SM) profiles and found that, in general, SMs increase with age in N2 animals (Figure 3B and Supplementary Figure 3). This was also found by Cutler et al. (2014) that analyzed SM levels from egg to 11-day adults [25]. However, our analysis was different as we did not directly examine the d17:1 iso-sphingoid base that is most prominent in *C. elegans* [45]. Of the SMs we identified, we found that *asm-3* mutants had higher total SMs compared to N2 at 1 day (*p*=0.03) but then was lower at 10 days compared to N2 (*p*<0.00001). In *C. elegans*, there are three acid sphingomyelinases genes (*asm-1, 2, 3*) and an uncharacterized neutral sphingomyelinase (T27F6.6). However, their adult expression patterns are unknown, and therefore, the different enzymes may differentially contribute to sphingolipid metabolism and total sphingomyelin levels throughout the worm's life. Indeed, *asm-1, asm-2*, and *asm-3* knockdown by RNAi lead to small increases in lifespan independently, and *asm-1* and *asm-2* knockdown by RNAi can further increase lifespan of *asm-3* mutants [24].

Of the SMs we observed, which are more similar to mammalian SMs, the largest increases observed in N2 animals from 1-day to 10-day adults are in several monosaturated sphingomyelins, specifically SM(24:1) ($\log_2$FC = 2.6, FDR=2.43e-28), SM(22:1) ($\log_2$FC = 1.9, FDR=4.54e-10) and SM(26:1) ($\log_2$FC = 1.6, FDR=2.10e-8). Intriguingly, SM(24:1) abundance is low at 1-day in both N2 and *hyl-2* mutants, and increases at both 5 and 10-days. However, in *asm-3* mutants, SM(24:1) abundance is low at 1-day, increases at 5-days, and then decreases again at 10-days. Furthermore, *asm-3* mutants exhibit different 10-to-1 day changes compared to N2; for example, whereas N2 show increases in the saturated sphingomyelins SM(16:0), SM(18:0), SM(22:0), *asm-3* show decreases (Supplementary Tables 3, 8). Interestingly, the saturated sphingomyelins SM(16:0) ($\log_2$FC=1.9, FDR=2.38e-8), SM(18:0) ($\log_2$FC=1.3, FDR=0.026), and SM(22:0) ($\log_2$FC=0.47, FDR=0.0293) show even greater increases from 1 to 10 days in *hyl-2* mutants than N2. Given the role of SMs on membrane fluidity, these age dependent changes may affect membrane properties in *asm-3* and *hyl-2* mutants that affect cell physiology.

To explore specific lipid changes associated with age, we next examined fold changes of each lipid molecule using volcano plots, plotting their concentration to their false discovery rate (FDR, or adjusted *p* value). Those lipids with greater than a 4-fold change ($\log_2$ FC > 2) are highlighted in Figure 4 (and Supplementary Tables 2–9). First, we examined changes in 10-day old N2 animals compared to 1-day old animals (10d/1d; Figure 4A); many of the lipids that are lower at 10 days compared to 1 day were LPCs, whereas many of the lipids that were higher at 10 days were triacylglycerols (Figure 4A). When examining changes in 5-day old N2 animals compared to 1-day animals, we observed similar changes in triacylglycerols, but not LPCs (Figure 4B). Next, we compared lipidomes of 10-day old animals of *hyl-2, asm-3, daf-16,* and *eat-2* backgrounds to that of wildtype 10-day animals (Figure 4C–4F). Strikingly, the lipid changes in *asm-3* to N2 were similar to that of the long-lived *eat-2* to N2. Most of the highly significant changes were found to be lower levels of TAGs. Indeed, *eat-2* animals exhibit reduced TAG levels by Nile Red, Oil red O, and Sudan black staining, as well as gas chromatography [46, 47]. On the other hand, the profile of lipid changes in *hyl-2* to N2 was similar to that of the short-lived *daf-16* to N2. Both 10-day old *hyl-2* and *daf-16* showed increases in LPCs compared to 10-day wildtype, sharing many common LPCs including LPC(16:1), LPC(18:3) and LPC(20:0).

Given the changes in LPCs, we visualized differences in LPC levels across all animals in a heatmap (Figure 3C). We find that *asm-3* and *eat-2* show normal levels of LPCs at younger ages, but have much lower levels of LPCs at 10-days old. On the other hand, *hyl-2* and *daf-16* show increased LPC levels at younger and older ages. In humans, elevated levels of LPCs in circulating low density lipoprotiens (LDLs) are associated with disease [48], and elevated LPC levels are observed in stress conditions, particularly inflammatory disease [49].

Saturated and unsaturated fatty acid changes in *hyl-2*/CER synthase and *daf-16*/FOXO mutants

Fatty acid chain desaturation has been of interest in aging because polyunsaturated fatty acids (PUFAs) may be more susceptible to oxidation and cellular damage, suggesting that high levels of PUFAs may be detrimental to health. Indeed, older animals have a decreased monosaturated fatty acid to polyunsaturated fatty acid (MUFA:PUFA) ratio, suggesting that there are more PUFAs, or less MUFAs, with age; in addition, long-lived animals generally have a higher MUFA:PUFA ratio compared to short-lived animals [35, 36, 50]. We analyzed TAG and FFA and found that the MUFA:PUFA ratio declined in older ages for all genotypes (Figure 5A). However, when we analyzed total PUFAs, we found that both *hyl-2* and *daf-16* mutants had higher amounts of PUFAs than 10-day N2

animals (Figure 5B, 3.46 fold and 3.22 fold, p<1.0e-7 respectively). Both *hyl-2* and *daf-16* had PUFA levels at 1 day comparable to N2, but PUFA levels continued to increase significantly at each timepoint. Both *asm-3* and *eat-2* had non-significant changes at 10 days compared to N2. The changes in MUFA:PUFA ratio in older

animals was not observed when we analyzed saturation levels in PC and PE (Figure 5B). However, we did find that *hyl-2* and *daf-16* mutants also had increased amounts of saturated lipids found in PC and PE (Figure 5D, 3.96 fold, and 5.28 fold increase respectively; $p<1.0e-7$ for both).
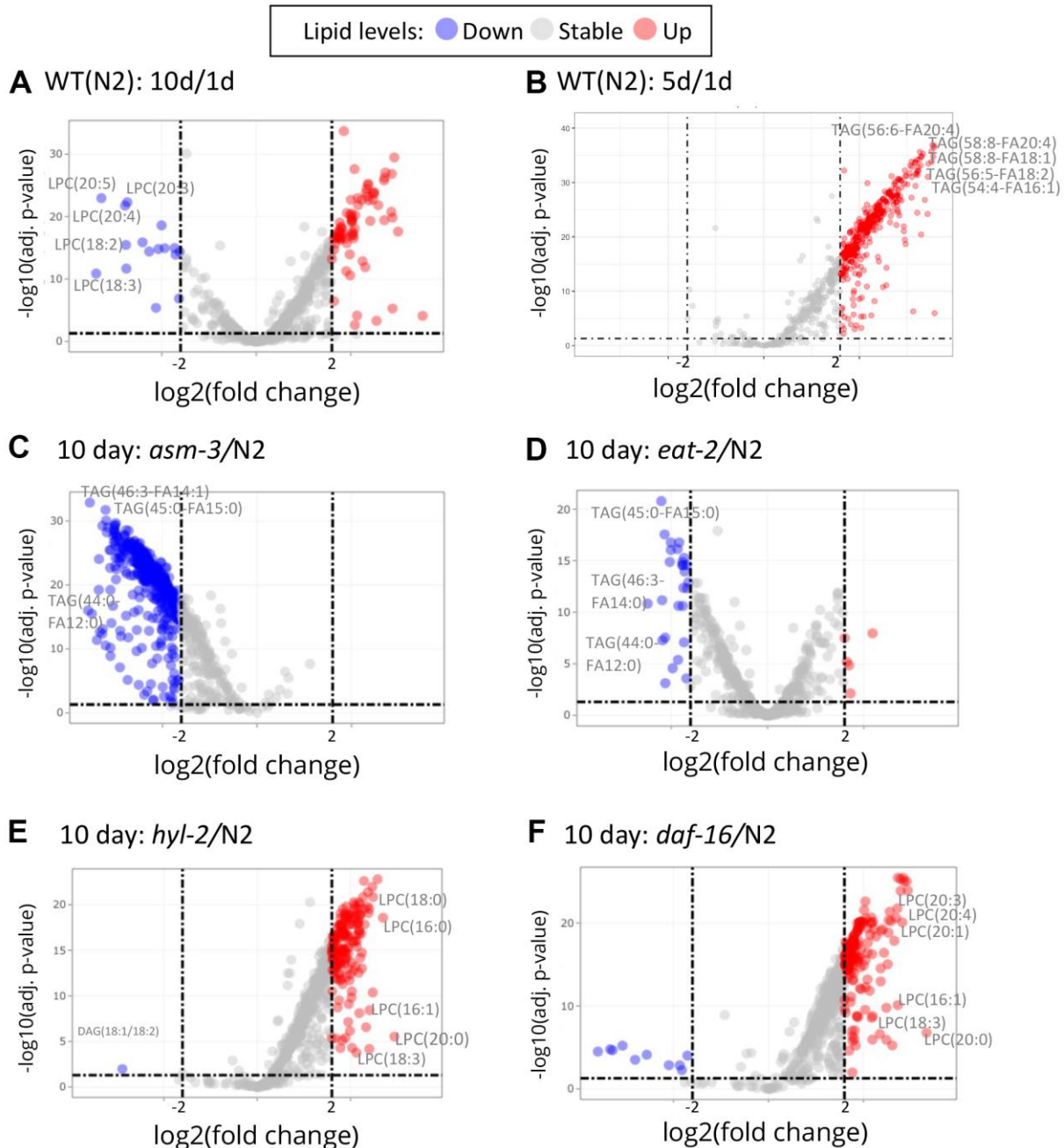
Figure 4. Volcano plots show that specific lipids change by age and genotype. Log₂ fold changes between groups are graphed by adjusted P values. Red indicates a greater than 2 log₂ fold increase of specific lipid, and blue indicates greater than -2 log₂ fold decrease (dashed lines). (**A**) Comparison of 10-day old N2 animals versus 1-day old N2 animals (10d/1d). 10-day old N2 animals have many decreased LPCs compared to 1-day. (**B**) Comparison of 5-day old N2 animals versus 1-day old N2 animals. (**C**) Comparison of 10-day old *asm-3* animals versus 10-day old N2 animals. (**D**) Comparison of 10-day old *eat-2* animals versus 10-day old N2 animals. (**E**) Comparison of 10-day old *hyl-2* animals versus 10-day old N2 animals. (**F**) Comparison of 10-day old *daf-16* animals versus 10-day old N2 animals.

Metabolic enzymes that produce elongated and desaturated fatty acids (Figure 1A) have been implicated in lifespan regulation [1, 13, 17, 31, 50]. Thus, we next explored whether aging affects gene expression of key enzymes in fatty acid lipid metabolism. Fatty acid metabolism starts with the fatty acid synthase FASN-1, which modifies malonyl-CoA to generate either C16 straight chain fatty acids by using Acetyl-CoA, or C13iso-branched fatty acid by using isovalaryl-CoA. From there, C16:0 can be elongated by fatty acid elongases or desaturated by fatty acid desaturases. We examined by qPCR whether elongases or desaturates are regulated by age or by mutations in *hyl-2* and *asm-3*. We found that two fatty acid elongases (*elo-1* and *elo-2*) did not change when comparing 1-day and 10-day old animals of any genotype (Figure 6A and Supplementary Table 10). When then analyzed fatty acid desaturases in the pathway (*fat-1*, *fat-2*, *fat-4*, *fat-6, and fat-7*). We found that 10-day old animals of all genotypes have very low expression of *fat-7*, which is a FA desaturase that converts FFA(18:0) to FFA(18:1). We did not observe changes in *fat-6* expression or other fatty acid desaturases examined.

C13:0iso-branched fatty acid leads to the synthesis of monomethyl branched chain fatty acids (mmBCFA), which are involved in growth and survival [51, 52]. ELO-5 and ELO-6 specifically transfer acyl groups to C13iso and C15iso fatty acids [51, 53]. We examined whether there were gene expression changes in *elo-5* and *elo-6* in 1- and 10-day old N2, *hyl-2*, and *asm-3* animals. Interestingly, *elo-5* showed significant decreases in wildtype and *hyl-2* animals, and non-significant changes in *asm-3* animals (Figure 6A). *hyl-2* further shows significant downregulation of *elo-6*. The downregulation of *elo-5* in N2 and *asm-3* animals may contribute to the lower levels of FFA(17:0) (Figure 6B). However, it is not clear why *hyl-2* mutants exhibit low expression of *elo-5* and *elo-6* despite sustained levels of FFA(17:0). It is possible some feedback mechanisms exist to decrease their expression, or that early steps in mmBCA synthesis are increased to affect sphingolipid metabolism in *hyl-2*. Indeed, many sphingomyelin species are higher in 10-day old *hyl-2* mutants (Figure 3B) compared to both 1-day *hyl-2* or N2 animals.

We found that the lipid levels of the FFA(15:0) and FFA(17:0) is increased in 10-day *hyl-2* (log$_2$FC=1.28,
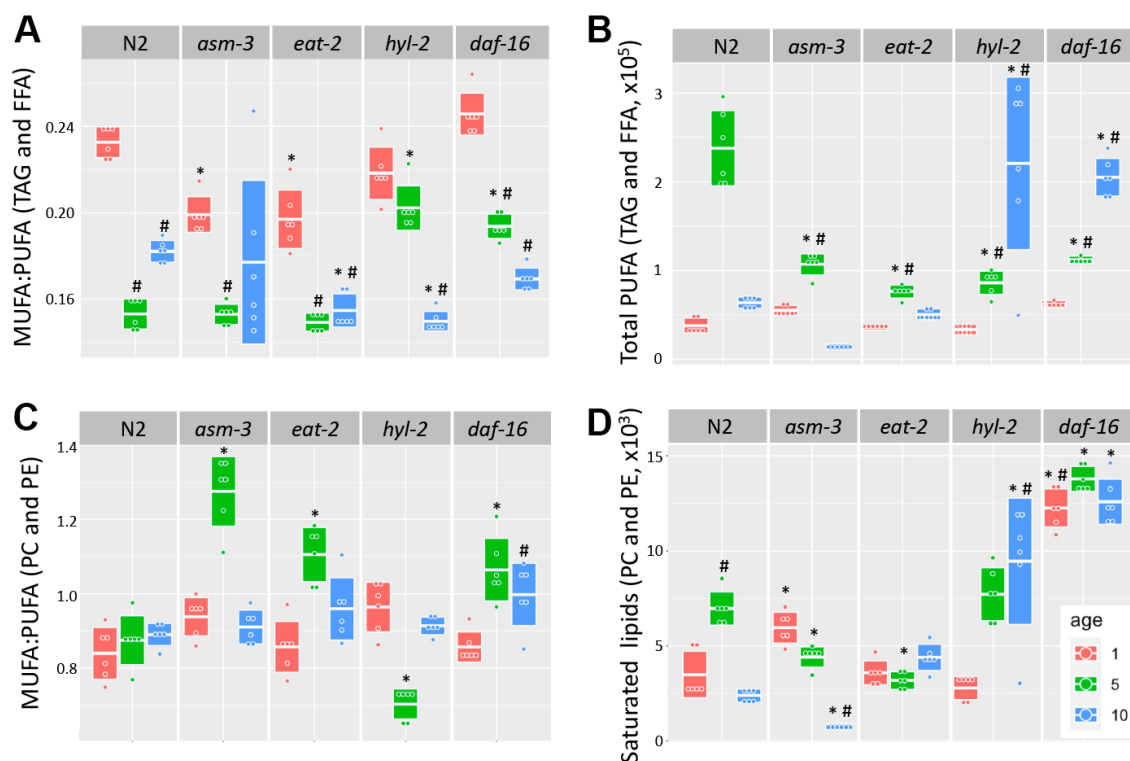
Figure 5. Analysis of acyl chain saturation during young and old *asm-3* and *hyl-2* mutants. Chain saturation was analyzed and compared between 1-day (red), 5-day (green), and 10-day (blue) old N2, *asm-3*, *eat-2*, *hyl-2*, and *daf-16* animals. Total (**A**) MUFA:PUFA ratios in TAG and FFA, (**B**) total polyunsaturated chains in in TAG and FFA, (**C**) MUFA:PUFA ratios in PC and PE, and (**D**) saturated PC and PE were summed for each group (n=6). Boxes in graphs represent the middle quartile for the data points in each group. For all, # indicates *p*<0.05 compared to 1-day counterpart and * indicates *p*<0.05 compared to N2 counterpart.

p=1.66e-10; Figure 6B) and *daf-16* (log$_2$FC=2.55, p=2.50e-23) mutants compared to N2. On the other hand, *asm-3* animals showed decreases in FFA(15:0) and FFA(17:0) (log$_2$FC=-1.98, p=1.10e-18) (Figure 6B). We were interested in whether the differences in these chains are also observed in triacylglycerols (TAGs). When analyzing FA15:0 and FA17:0 chains that are part of TAGs in *asm-3* animals, we found that they also exhibited decreased TAGs containing FA15:0 and FA17:0 at 10-day compared to 1-day; *hyl-2* mutants showed a general increase in in these TAGs compared to N2, but not in either specific day (Supplementary Figure 4). Although our lipidomics detection could not identify the iso-branched species specifically, this suggests that *hyl-2* might have higher mmBCFAs at older ages, whereas *asm-3* mutants have lower.

To determine whether sphingolipid metabolism itself is altered by age, we examined key enzymes in the production of sphingolipids from mmBCFAs. The mmBCFA C15iso and C17iso fatty acids can be made into C17iso-sphinganine or its precursors through serine palmitoyl transferase (*sptl-1*) in *C. elegans* (Figure 1A) [54, 55]. We found that *sptl-1/*serine palmitoyltransferase does not change with age or strain (Figure 6A). The

addition of fatty acid to C17iso-sphinganine to make dihydroceramide is mediated by *hyl-2*, as well as other ceramide synthases (Figure 1A). *hyl-2* specifically transfers fatty acids of shorter chains (C20-22) [40]. We further explored gene expression changes of *hyl-2* and *asm-3* itself, and found that *asm-3* showed a trend to decrease in N2 animals at 10-days compared to 1-day (Figure 6A). However, we observed that, in general, *asm-3* had low expression in all genotypes at 10-days. Interestingly, there was a large 10-day to 1-day decrease in *asm-3* expression observed in *hyl-2* animals. Thus, it is possible that *hyl-2* animals, and old animals in general, have reduced breakdown of sphingomyelin at older ages that contribute to their poor stress response and reduced lifespan. However, given that *asm-3* mutants have increased lifespan, it is not clear how reduced *asm-3* expression at later ages may specifically modify aging processes differently than complete knockouts. Together, these data support a model where increased abundance of sphingolipid precursors and sphingomyelin may contribute to poor aging phenotypes. Indeed, our findings support lipidomic analyses of human longevity suggesting that centenarians upregulate mechanisms to upregulate sphingomyelins to ceramide-containing glycosphingolipids [56, 57].
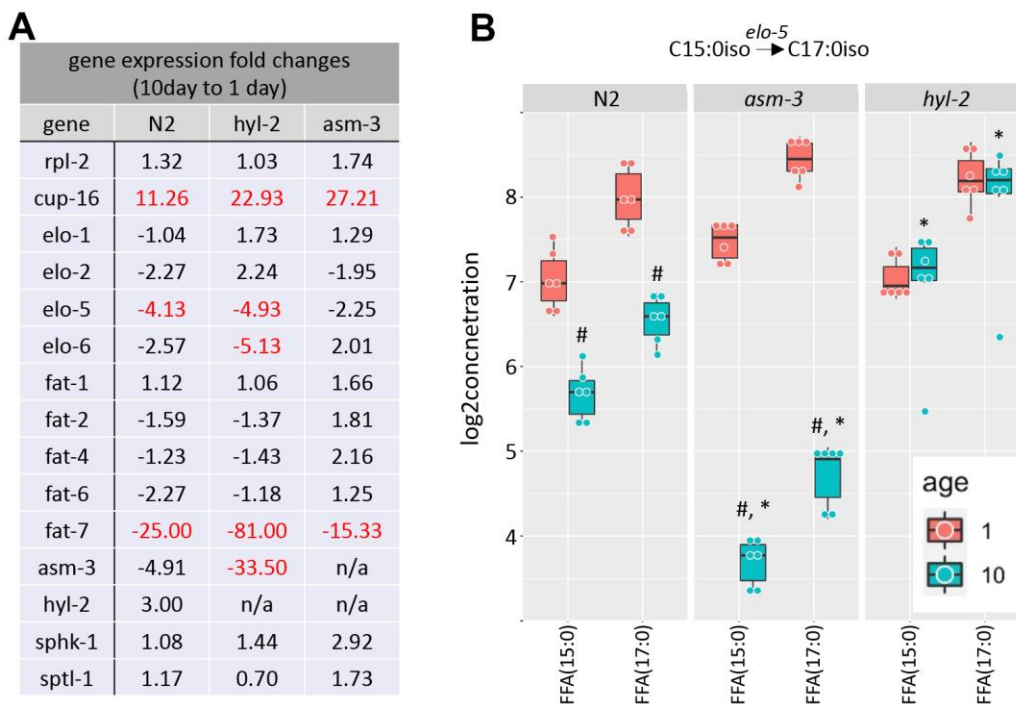
Figure 6. Saturated and polyunsaturated fatty acids metabolism. (**A**) Table of gene expression for fatty acid for elongases and desaturates examined in 1-day and 10-day old N2, *asm-3,* and *hyl-2* animals by quantitative PCR. Data are represented by 2^{-ddCT} fold change of 10-day N2 compared to 1-day values (n=3 for each group, red indicates fold changes that are *p*<0.01). The reference gene was *rps-2*, and *rpl-2* and *cup-16* are control genes known to remain unchanged and increase, respectively, in older animals. (**B**) Log$_2$ concentrations of FFA(15:0) and FFA(17:0) are shown at 1- and 10-day old N2, *asm-3*, and *hyl-2* animals (n=6 for each group). For all, #indicates *p*<0.05 compared to 1-day counterpart of the same genotype. *indicates *p*<0.05 compared to N2 counterpart of the same age.

DISCUSSION

Ceramide synthase and sphingomyelinase are enzymes in sphingolipid metabolism that impact sphingomyelin and ceramide levels and aging. We examined lipidomes of mutants for these sphingolipid metabolism enzymes in *C. elegans* and observed lipid changes that may begin to elucidate how sphingolipid alterations might alter broad lipid composition. We found that *hyl-2*/CER synthase mutants have poor stress response and have many similar lipidomic changes as the short-lived *daf-16*/FOXO mutant. These include increased total PUFAs and increases in specific LPCs. Conversely, *asm-3*/acid sphingomyelinase mutants have slight resistance to oxidative stress and have lipidomic changes more similar to the long-lived *eat-2*/mAChR model. Further analyses of specific lipid changes may provide insight into how these sphingolipid mutants may mediate stress response and aging. As lipid composition changes with age, better understanding of lipid signatures in mutant models may become useful for aging studies.

Sphingolipid metabolism changes associated with aging

Sphingolipids are gaining attention in their roles in aging but have diverse and complex functions in cells. Sphingomyelins (SM) are among the most prevalent lipids found on cell membranes, and they influence membrane fluidity and cell signaling. We found that most SMs increase with age in general, and *asm-3*/acid SMase mutants had differing SM profiles than N2. Specifically, 10-day old wild type animals have increased longer chained SMs. While our study did not examine the more abundant d17:1 sphingoid species of SM, our finding supports previous studies of SM changes with age, which show that wildtype animals generally have greater SM elongation (increase C22:0 and C24:0 in 11-day adults compared to 3-day adults) and desaturation (less C18:0) [25]. Longer acyl chained SM create interdigitating acyl chains, which can reduce membrane mobility, and may contribute to the decrease in membrane fluidity observed in aging animals and senescent cells [58–60]. Interestingly, blood serum sphingomyelin is elevated with age and is associated with Alzheimer's disease [61]. In addition, in the Baltimore longitudinal study, Mielke et al. (2014) found that most SMs increase with age, particularly in female subjects; however, some longer chained saturated SMs (C20:0, C22:0 and C24:0) increase in early aging but may decrease with late age (>70years old) [22]. Saturated sphingomyelins also appear correlated with obesity and insulin resistance [62].

Why might changes in sphingolipid metabolism cause alterations in adult stress response and lifespan? Ceramides, which can be produced by synthesis (ceramide synthases) or recycling through sphingomyelin (sphingomyelinases), have been found to be important for anoxia, autophagy, mitochondrial stress response, locomotion and others in *C. elegans* [38, 40, 63, 64]. Thus, it is likely that altered activity of enzymes such as ceramide synthases and acid sphingomyelinases serve broad roles in aging physiology. More studies showing direct impact of lipid changes will help elucidate how sphingolipids may mediate cellular processes associated with aging. For example, Wang et al. (2021) show that glucosylceramides mediate clathrin binding to autophagolysosome for lysosome recycling. Furthermore, SM levels and ASM-3 function have been associated with insulin receptors signaling, suggesting that loss of specific SM may reduce or alter receptor abundance or localization [24, 61, 65]. Indeed, Kim and Sun (2012) show that mutations or pharmacological inhibition decreasing *asm-3* function increases lifespan and possibly through altered localization of the DAF-2/insulin-like receptors, or downstream targets, that are associated with stress response and aging in worms. However, the specific sphingomyelins species were not examined in these studies, and further characterization of specific carbon length and saturation may provide greater insight into mechanisms of sphingomyelin regulation of aging. On the other hand, studies on Drosophila *cpes* mutants, which have reduced ceramide phosphoethanolamine (CPE) – a structural analog of mammalian sphingomyelin – show that CPE has a positive correlation to lifespan increase; specifically, the presence of CPE on glial membranes alters circadian rhythms, glutamate homeostasis and shortens lifespan [66]. Furthermore, sphingolipids on synaptic vesicles have been shown to mediate SNARE proteins and exocytosis [67]. Thus, changes in SMs may alter specific organelle and cell membrane composition that impacts local protein-lipid interactions.

Interestingly, we found that *asm-3* gene expression decreases with age, suggesting that sphingomyelin breakdown and broad lipid profiles may change during aging. Indeed, examining SM show that SMs increase with age, and are higher in short-lived animals. However, lipid profiles may be highly specific to the organism, as higher sphingolipid saturation overall was also observed in other long-living species [3]. It is worth noting that there are also race specific effects, as higher levels of sphingomyelins are observed in African Americans and Hispanics when compared to Caucasians [22, 68]. Thus, the changes in SMs are complex, and may involve specific lipids, interactions with other factors and protein functions. Though not definitive, studies suggest that specific sphingomyelins, and enzymes that alter carbon length or saturation, may play important roles in maintaining membrane sphingolipid composition important for many receptors or proteins associated with aging.

Fatty acids associated with fat storage and lipid oxidation

Free fatty acids (FFA) serve roles in both fat storage and membrane lipid composition. Fat storage is important for cellular energy and can change with age, but there is not a direct correlation between lipid levels and lifespan [69]. The dietary restriction mutant model *eat-2* has lower fats in storage whereas the insulin signaling model *daf-2(*e1370*)* has high levels of TAG; yet both are long-lived [37, 41, 69–72]. Furthermore, effects may even be genotype dependent, as not all *daf-2* mutant alleles share the higher TAG phenotype (Perez and Van Gilst 2008). However, higher TAG have been proposed to contribute to the longer lifespans of animals due to the greater reserve of stored fats for energy utilization in late life [13]. In other model organisms such as yeast, deletion of triglyceride lipases results in increased lipid accumulation as well as increased lifespan [18, 73].

Lipid droplets (LD) contain stored triacylglycerols, and these TAGs are broken down by enzymes that mediate lipophagy to make free fatty acids [16]. This process may involve autophagy genes as well as the lipase *lipl-4* in *C. elegans* [74, 75]. Indeed, *lipl-4* is required for the long lifespan phenotype of *daf-2* mutants [76]. Interestingly, glycosphingolipids have recently been shown to mediate clathrin-dependent lysosome formation during autophagy, and increased autophagy in the long-lived *hyl-1;lagr-1* ceramide synthase mutants (which produce longer chained ceramides) is abolished by loss of *atg-12* [34, 63]. Thus, it is intriguing to speculate that changes in sphingolipid metabolism may mediate membrane dynamics that facilitate lipophagy. Indeed, acid sphingomyelinase (aSMase) is found in lysosomes, and *asm-3*/acid SMase is involved in lipid storage in embryos and may have roles in general lipid metabolism [77, 78]. However, Nile Red staining, which might more specifically label lysosomal lipids, did not show broad changes in lipids levels.

Fatty acids also make up more complex lipids that are part of cell and organelle membranes. The oxidative theory of aging suggests that increased lipids, such as polyunsaturated fatty acids (PUFAs), are more susceptible to oxidation and can lead to cell damage during aging [79, 80]. Indeed, elevated levels of PUFAs appear to increase oxidation and cell damage, and low PUFA levels correlate to longevity in mammals and worms [10, 50]. In *C. elegans*, PUFAs comprise 46% of total fatty acids of phospholipids but only 12% of triacylglycerols, suggesting that a greater percent of fatty acids is found in phospholipids than triacylglycerols [31]. We found that *hyl-2/*CER synthase and shorter lived *daf-16* have higher amounts of many PUFAs, and this may contribute to their poor lifespan and healthspan in these animals. Many long-lived worms also have increases in MUFA:PUFA ratios, suggesting that there are less polyunsaturated fatty acids available for oxidative damage. Indeed, mutations in Δ9 desaturases (*fat-5*, *fat-6*, and *fat-7*), which produces PUFAs in *C. elegans*, or supplementation of the PUFA eicosapentaenoic acid (EPA) shortens lifespan [50]. However, ω-6 PUFAs has also been shown increase autophagy and extend lifespan [81]. This discrepancy is observed elsewhere as a study showed that centenarians increase ω-3 to ω-6 PUFAs [82]. Furthermore, long-lived *daf-2* mutants have lower expression of *fasn-1*, a fatty acid synthase important for the initial steps of fatty acid production [83]. This may suggest a downregulation of the metabolic processes associated with fatty acid production, elongation, or desaturation mediates the effects of lipid metabolism on aging.

Phylogenomic studies have also identified evolutionary targets that link metabolic enzymes to longevity and include genes with functions in fatty acid elongation and desaturation [30]. We found that age decreases the expression of *elo-5*, which produces C15iso lipids and is important for development [51]. Interestingly, the long-lived phenotype of *daf-2* is somewhat dependent on *elo-5* [84]. We found that *hyl-2* and *daf-16* have increased levels of longer chained PUFAs at 10-days, compared to wildtype animals, suggesting that fatty acid metabolism in these animals may be increased. Shmookler-Reis (2011) also suggests that elongase activity negatively correlates with aging; specifically, the combined regulation for increased Δ9-desaturase activity to generate MUFAs, and decreased activity of downstream Δ5-desaturases that generate PUFAs, may correlate with longevity.

Different methodologies to lipid extractions can yield changes in lipid composition. We note that our protocol called for thawing frozen samples prior to lipidomics sample preparation. This freeze and thaw have been previously done on *C. elegans* for lipidomics [36, 85], and our quality control does not suggest degradation of any particular class of lipids. However, others have prepped from frozen C. elegans extracts directly [31]. Different tissue treatment conditions can damage tissues and result in elevations in FFA within samples [44]. Thus, total FFA and LPC levels may be impacted by sample preparation methods, although we do not suspect changes in relative values between genotypes emphasized in this analysis.

Lysophosphatidylcholines are increased in short-lived animals

High levels of LPCs may mediate cell stress. We found that LPCs were more abundant in short-lived mutants, *hyl-2*/CER synthase and *daf-16*/FOXO. LPCs can

increase reactive oxygen species in aortic endothelial cells [86]. In addition, osmotic stress was shown to increase the production of LPC through *daf-16*, and that LPC(18:0) specifically caused osmotic stress mediated embryonic lethality [87]. Furthermore, *daf-2*/insulin-like receptor mutants exhibit 50% lower levels of LPCs compared to the wild type, including LPC(18:0) and PUFA containing LPCs (20:5, 20:4, and 20:3) [37]. In addition, Rebaudioside A, a sweetener that decreased ROS accumulation and improved oxidative stress response, caused decreased levels of LPC(20:4) and LPC(20:5) [88]. Intriguingly, human studies also show that LPC(20:3) and LPC(20:4) are lower in elderly [19]. On the other hand, others have shown that low levels of LPCs have also been linked to poor mitochondrial function [1]. Together, these data may suggest that regulation of LPC content may mediate mitochondrial function and oxidative stress in animals, and that low or high LPCs may affect healthspan or lifespan.

In summary, analyzing lipidomes of models of aging has the potential to identify cellular processes and signaling pathways important for animal stress response and aging. We found here that *C. elegans hyl-2*/CER synthase mutants had a 10-day lipid profile that mirrored shorter lived *daf-16*/FOXO mutants, which included elevated PUFAs and LPCs. Age caused increased sphingomyelin levels, particularly in short-lived animals. This may suggest that the regulation of sphingolipid metabolism may mediate changes in cell structure and function important for healthy aging. Future studies connecting lipidomic changes in sphingolipid metabolism mutants to mechanistic changes in cells of mutant models will be important next steps to better understanding the roles of sphingolipids in aging.

MATERIALS AND METHODS

C. elegans strains

All *C. elegans* were grown on nematode growth media (NGM) at 20° C methods (Stiernagle 2006). Plates were seeded with OP50 *E. coli*. For lifespan and aging studies, NGM plates were supplemented with 50μM 5-Fluoro-2′-deoxyuridine (FUdR, Alfa Aesar). The following strains were provided by the CGC, which is funded by NIH Office of Research Infrastructure Programs (P40 OD010440): *hyl-2(gnv1), asm-3(ok1744)*, *eat-2(ad1113),* and *daf-16(mu86)*. The wildtype strain used was N2 Bristol. All strains were outcrossed at least 4x.

Oxidative stress assays

For stress assays, *N2*, *hyl-2(gnv-1),* and *asm-3(ok1744)* animals were synchronized via egg lay on NGM plates seeded with OP50 *E. coli*. When progeny reached the L4 stage, animals were washed with M9 and transferred to NGM/OP50 plates supplemented with 50μM FUdR. For acute juglone assays, animals were grown to 1-, 5-, and 10-day adults. At these ages, approximately 50 adult worms per genotype were transferred to 150μM juglone (Sigma Aldrich) in M9 by placing 10-15 animals per well for 4 wells, in a 96 well plate [89]. Worms were scored for survival every two hours for 8 hours. Animals were considered dead if they did not respond to agitation. Data was analyzed using Kaplan-Meier estimates and log-rank tests, with Bonferroni correction, in the R statistical package *survival* and *survminer*.

Nile red staining and imaging

To generate a synchronous population of worms, adult N2, *hyl-2(gnv1),* and *asm-3(ok1744)* animals were allowed to lay eggs for 4-6 hours on NGM plates seeded with OP50 *E. coli*. When progeny reached the L4 stage, they were moved onto OP50 *E. coli* seeded NGM plates supplemented with 50μM FUdR. At 1-day or 10-days after the L4 stage, animals stained with Nile Red as previously described previously [42]. Briefly, animals were washed with PBST, incubated in 40% isopropanol of 3 minutes, stained with Nile Red working solution (30μg/mL 40% isopropanol) for 2 hours, in the dark, shaking at room temperature. After incubation, worms were washed again with PBST in the dark for 30 minutes and worms were moved to a slide for imaging. Worms were imaged using an ECHO Revolve R4 microscope equipped with Olympus UPlan Fluorite objectives in the FITC/GFP channel. Images were then analyzed using ImageJ version 1.53e [90]. Whole worm fluorescence were used for statistical analysis, accounting for background fluorescence, and values were analyzed by two-way ANOVA and Tukey post-hoc tests in the R Statistical Package.

RNA isolation and real time quantitative polymerase chain reaction

N2, *hyl-2(gnv1),* and *asm-3(ok1744)* animals were synchronized using a standard egg prep protocol and distributed onto NGM plates supplemented with OP50. Once animals reached the L4 stage, they were transferred to NGM plates supplemented with 50μM FUdR and seeded with OP50. Approximately 500 worms per biological replicate were collected at 1 day and 10 days past the L4 stage and flash frozen using liquid nitrogen. RNA was isolated using TRIZOL (Sigma Aldrich) and chloroform extraction and then stored at -80° C. The absorbance at 260/280nm was measured using a NanoDrop Spectrophotometer (Thermo Fisher Scientific) to determine the purity of the RNA. cDNA was generated

from ~500ng/µL of total RNA using the QuantiNova Reverse Transcription Kit (Qiagen). In the first step of the cDNA synthesis, all RNA was treated with a gDNA removal step to remove gDNA contamination. Quantitative, real-time polymerase chain reaction was performed in triplicate using the QuantiNova SYBR Green PCR Kit and Rotor Gene Q (Qiagen). mRNA fold changes were calculated using ddCT method (Wu, Tian et al. 2020). mRNA levels of the genes of interest were compared with the mRNA levels of the reference gene *rps-2*. Gene expression by qPCR was repeated with biological replicates and three technical replicates. All qPCR primers (Supplementary Table 1) were designed to be intron spanning, and one primer from each set was intron bridging to reduce the likelihood of gDNA amplification. Data were analyzed by two-way ANOVA and Tukey post-hoc tests in the R Statistical Package.

Sample preparation for lipidomics

Approximately 1000 *C. elegans* worms were synchronized by treating gravid adults with an alkaline hypochlorite solution (bleach/NaOH). Worms were then grown to L4 stage and transferred to NGM agar plates containing 50µM FUdR. Worms were then collected after 1, 5, and 10 days. Six replicate samples of each group were then sent for lipidomics analysis at the Northwest Metabolomics Research Center (University of Washington).

C. elegans samples were prepared as described (Hanson et al., 2020). Briefly, frozen worm samples were thawed and vortexed; 250µL of worm slurry was transferred to a borosilicate glass culture tube (16 × 100 mm). Next, 250µL of water, 1 mL of methanol, and 450µL of dichloromethane were added to all samples. Then, 25µL of the isotope labeled internal standards mixture were added and incubated at room temperature for 30 min. Next, another 500µL of water and 450µL of dichloromethane were added to the tube and centrifuged at 2500×g at 15° C for 10 min. The bottom organic layer was transferred to a new tube and 900µL of dichloromethane was added to the original tube for a second extraction. The combined extracts were concentrated under nitrogen and reconstituted in 250µL of the running solution (10mM ammonium acetate in 50:50 methanol:dichloromethane).

Mass spectrometry

C. elegans samples were analyzed as described by [91] and completed at the Northwest Metabolomics Research Center. Briefly, Quantitative lipidomics was performed with the Sciex Lipidyzer platform consisting of a Sciex QTRAP® 5500 mass spectrometer equipped with SelexION® for differential mobility spectrometry

(DMS). 1-propanol was used as the chemical modifier for the DMS. Samples were introduced to the mass spectrometer by flow injection analysis at 8 µL/min. Each sample was injected twice, once with the DMS on (PC/PE/LPC/LPE/SM), and once with the DMS off (CE/CER/DAG/DCER/FFA/HCER/ LCER/TAG). The lipid molecular species were measured using multiple reaction monitoring (MRM) and positive/negative polarity switching. A total of 1070 lipids and fatty acids were targeted in the analysis. Using 54 internal standards previously used and described in [92], quantities (in µmol/g) of each lipid species could be calculated. Data were acquired and processed using Analyst 1.6.3 and Lipidomics Workflow Manager 1.0.5.0.

Data processing and statistical analyses

Statistical analysis was carried out using R (version 3.6.0). The targeted lipidomic assay was designed to detect 1070 lipid species. Data were in concentration per worm weight (nmol/g of worm tissue (μM)), and therefore no further normalization was performed prior to statistical analysis. Only lipids in which missing data across all groups were less than 20% were included in further analysis. Out of the possible 1071 lipid species that the assay could detect, 701 lipids passed these filtering criteria and were included in further analysis. We used a quantile regression approach for the imputation of left-censored missing data (QRILC), which has been suggested as the favored imputation method for left-censored MNAR data [93]. This was implemented in the R imputeLCMD package.

We fit linear models to the lipidomic data using the Bioconductor limma package [94] to assess the difference in abundance between experimental groups. The limma package uses empirical Bayes moderated statistics, which improves power by 'borrowing strength' between features in order to moderate the residual variance [95]). We selected lipids with a false discovery rate (FDR) of 5%.

In the heatmaps, z-scores are calculated by adjusting the data, by feature, to have a mean of zero and a standard deviation of 1. The heatmaps were generated using the R statistical package. For direct comparisons of specific lipids between strains, $\log_2$ concentrations were compared between samples using a two-way ANOVA and Tukey post hoc analyses in the R statistical package.

AUTHOR CONTRIBUTIONS

JC conceived all experiments, collected and analyzed data, and wrote and edited the manuscript. TS and GM performed qPCR experiments and edited the manuscript. TS had additional roles in conceiving the

experimental design and analyzing data. JR performed lipidomics sample collection, LB and DR performed sample preparations for lipid mass spectrometry, LW performed lipidomic analyses, and AK, GM, MG, MP, and SB performed physiological experiments.

CONFLICTS OF INTEREST

The authors declare that the research was conducted in the absence of any commercial or financial relationships that could be construed as a potential conflicts of interest.

REFERENCES

1. Johnson AA, Stolzing A. The role of lipid metabolism in aging, lifespan regulation, and age-related disease. Aging Cell. 2019; 18:e13048.
   https://doi.org/10.1111/acel.13048
   PMID:31560163

2. Jové M, Mota-Martorell N, Pradas I, Galo-Licona JD, Martín-Gari M, Obis È, Sol J, Pamplona R. The Lipidome Fingerprint of Longevity. Molecules. 2020; 25:4343.
   https://doi.org/10.3390/molecules25184343
   PMID:32971886

3. Bozek K, Khrameeva EE, Reznick J, Omerbašić D, Bennett NC, Lewin GR, Azpurua J, Gorbunova V, Seluanov A, Regnard P, Wanert F, Marchal J, Pifferi F, et al. Lipidome determinants of maximal lifespan in mammals. Sci Rep. 2017; 7:5.
   https://doi.org/10.1038/s41598-017-00037-7
   PMID:28127055

4. Graessler J, Schwudke D, Schwarz PE, Herzog R, Shevchenko A, Bornstein SR. Top-down lipidomics reveals ether lipid deficiency in blood plasma of hypertensive patients. PLoS One. 2009; 4:e6261.
   https://doi.org/10.1371/journal.pone.0006261
   PMID:19603071

5. Han X, Rozen S, Boyle SH, Hellegers C, Cheng H, Burke JR, Welsh-Bohmer KA, Doraiswamy PM, Kaddurah-Daouk R. Metabolomics in early Alzheimer's disease: identification of altered plasma sphingolipidome using shotgun lipidomics. PLoS One. 2011; 6:e21643.
   https://doi.org/10.1371/journal.pone.0021643
   PMID:21779331

6. Hu C, Kong H, Qu F, Li Y, Yu Z, Gao P, Peng S, Xu G. Application of plasma lipidomics in studying the response of patients with essential hypertension to antihypertensive drug therapy. Mol Biosyst. 2011; 7:3271–9.
   https://doi.org/10.1039/c1mb05342f PMID:22009255

7. Naudí A, Cabré R, Jové M, Ayala V, Gonzalo H, Portero-Otín M, Ferrer I, Pamplona R. Lipidomics of human brain aging and Alzheimer's disease pathology. Int Rev Neurobiol. 2015; 122:133–89.
   https://doi.org/10.1016/bs.irn.2015.05.008
   PMID:26358893

8. Stoessel D, Schulte C, Teixeira Dos Santos MC, Scheller D, Rebollo-Mesa I, Deuschle C, Walther D, Schauer N, Berg D, Nogueira da Costa A, Maetzler W. Promising Metabolite Profiles in the Plasma and CSF of Early Clinical Parkinson's Disease. Front Aging Neurosci. 2018; 10:51.
   https://doi.org/10.3389/fnagi.2018.00051
   PMID:29556190

9. Meikle TG, Huynh K, Giles C, Meikle PJ. Clinical lipidomics: realizing the potential of lipid profiling. J Lipid Res. 2021; 62:100127.
   https://doi.org/10.1016/j.jlr.2021.100127
   PMID:34582882

10. Jové M, Naudí A, Aledo JC, Cabré R, Ayala V, Portero-Otin M, Barja G, Pamplona R. Plasma long-chain free fatty acids predict mammalian longevity. Sci Rep. 2013; 3:3346.
    https://doi.org/10.1038/srep03346 PMID:24284984

11. Jové M, Naudí A, Gambini J, Borras C, Cabré R, Portero-Otín M, Viña J, Pamplona R. A Stress-Resistant Lipidomic Signature Confers Extreme Longevity to Humans. J Gerontol A Biol Sci Med Sci. 2017; 72:30–7.
    https://doi.org/10.1093/gerona/glw048
    PMID:27013396

12. Almeida I, Magalhães S, Nunes A. Lipids: biomarkers of healthy aging. Biogerontology. 2021; 22:273–95.
    https://doi.org/10.1007/s10522-021-09921-2
    PMID:33837874

13. Mutlu AS, Duffy J, Wang MC. Lipid metabolism and lipid signals in aging and longevity. Dev Cell. 2021; 56:1394–407.
    https://doi.org/10.1016/j.devcel.2021.03.034
    PMID:33891896

14. Pamplona R. Membrane phospholipids, lipoxidative damage and molecular integrity: a causal role in aging and longevity. Biochim Biophys Acta. 2008; 1777:1249–62.
https://doi.org/10.1016/j.bbabio.2008.07.003
PMID:18721793

15. Hansen M, Flatt T, Aguilaniu H. Reproduction, fat metabolism, and life span: what is the connection? Cell Metab. 2013; 17:10–9.
https://doi.org/10.1016/j.cmet.2012.12.003
PMID:23312280

16. Kounakis K, Chaniotakis M, Markaki M, Tavernarakis N. Emerging Roles of Lipophagy in Health and Disease. Front Cell Dev Biol. 2019; 7:185.
https://doi.org/10.3389/fcell.2019.00185
PMID:31552248

17. Bustos V, Partridge L. Good Ol' Fat: Links between Lipid Signaling and Longevity. Trends Biochem Sci. 2017; 42:812–23.
https://doi.org/10.1016/j.tibs.2017.07.001
PMID:28802547

18. Li X, Handee W, Kuo MH. The slim, the fat, and the obese: guess who lives the longest? Curr Genet. 2017; 63:43–9.
https://doi.org/10.1007/s00294-016-0617-z
PMID:27230908

19. Yang S, Dong Y, Liu Y, Yan X, Sun G, Jia G, Li X, Liu H, Su H, Li Y. Application of lipidomics strategy to explore aging-related biomarkers and potential anti-aging mechanisms of ginseng. Biogerontology. 2021; 22:589–602.
https://doi.org/10.1007/s10522-021-09937-8
PMID:34542790

20. Gonzalez-Covarrubias V, Beekman M, Uh HW, Dane A, Troost J, Paliukhovich I, van der Kloet FM, Houwing-Duistermaat J, Vreeken RJ, Hankemeier T, Slagboom EP. Lipidomics of familial longevity. Aging Cell. 2013; 12:426–34.
https://doi.org/10.1111/acel.12064 PMID:23451766

21. Montoliu I, Scherer M, Beguelin F, DaSilva L, Mari D, Salvioli S, Martin FP, Capri M, Bucci L, Ostan R, Garagnani P, Monti D, Biagi E, et al. Serum profiling of healthy aging identifies phospho- and sphingolipid species as markers of human longevity. Aging (Albany NY). 2014; 6:9–25.
https://doi.org/10.18632/aging.100630
PMID:24457528

22. Mielke MM, Bandaru VV, Han D, An Y, Resnick SM, Ferrucci L, Haughey NJ. Factors affecting longitudinal trajectories of plasma sphingomyelins: the Baltimore Longitudinal Study of Aging. Aging Cell. 2015; 14:112–21.
https://doi.org/10.1111/acel.12275
PMID:25345489

23. Braun F, Rinschen MM, Bartels V, Frommolt P, Habermann B, Hoeijmakers JH, Schumacher B, Dollé ME, Müller RU, Benzing T, Schermer B, Kurschat CE. Altered lipid metabolism in the aging kidney identified by three layered omic analysis. Aging (Albany NY). 2016; 8:441–57.
https://doi.org/10.18632/aging.100900
PMID:26886165

24. Kim Y, Sun H. ASM-3 acid sphingomyelinase functions as a positive regulator of the DAF-2/AGE-1 signaling pathway and serves as a novel anti-aging target. PLoS One. 2012; 7:e45890.
https://doi.org/10.1371/journal.pone.0045890
PMID:23049887

25. Cutler RG, Thompson KW, Camandola S, Mack KT, Mattson MP. Sphingolipid metabolism regulates development and lifespan in Caenorhabditis elegans. Mech Ageing Dev. 2014; 143:9–18.
https://doi.org/10.1016/j.mad.2014.11.002
PMID:25437839

26. Cutler RG, Mattson MP. Sphingomyelin and ceramide as regulators of development and lifespan. Mech Ageing Dev. 2001; 122:895–908.
https://doi.org/10.1016/s0047-6374(01)00246-9
PMID:11348657

27. Hannun YA, Obeid LM. Principles of bioactive lipid signalling: lessons from sphingolipids. Nat Rev Mol Cell Biol. 2008; 9:139–50.
https://doi.org/10.1038/nrm2329
PMID:18216770

28. Bieberich E. Sphingolipids and lipid rafts: Novel concepts and methods of analysis. Chem Phys Lipids. 2018; 216:114–31.
https://doi.org/10.1016/j.chemphyslip.2018.08.003
PMID:30194926

29. Sacket SJ, Chung HY, Okajima F, Im DS. Increase in sphingolipid catabolic enzyme activity during aging. Acta Pharmacol Sin. 2009; 30:1454–61.
https://doi.org/10.1038/aps.2009.136
PMID:19749786

30. Jobson RW, Nabholz B, Galtier N. An evolutionary genome scan for longevity-related natural selection in mammals. Mol Biol Evol. 2010; 27:840–7.
https://doi.org/10.1093/molbev/msp293
PMID:19955481

31. Brock TJ, Browse J, Watts JL. Fatty acid desaturation and the regulation of adiposity in Caenorhabditis elegans. Genetics. 2007; 176:865–75.
https://doi.org/10.1534/genetics.107.071860
PMID:17435249

32. Obeid LM, Hannun YA. Ceramide, stress, and a "LAG" in aging. Sci Aging Knowledge Environ. 2003; 2003:PE27.
https://doi.org/10.1126/sageke.2003.39.pe27
PMID:14523222

33. Kraut R. Roles of sphingolipids in Drosophila development and disease. J Neurochem. 2011; 116:764–78.
https://doi.org/10.1111/j.1471-4159.2010.07022.x
PMID:21214556

34. Mosbech MB, Kruse R, Harvald EB, Olsen AS, Gallego SF, Hannibal-Bach HK, Ejsing CS, Færgeman NJ. Functional loss of two ceramide synthases elicits autophagy-dependent lifespan extension in C. elegans. PLoS One. 2013; 8:e70087.
https://doi.org/10.1371/journal.pone.0070087
PMID:23894595

35. Schroeder EA, Brunet A. Lipid Profiles and Signals for Long Life. Trends Endocrinol Metab. 2015; 26:589–92.
https://doi.org/10.1016/j.tem.2015.08.007
PMID:26439976

36. Wan QL, Yang ZL, Zhou XG, Ding AJ, Pu YZ, Luo HR, Wu GS. The Effects of Age and Reproduction on the Lipidome of *Caenorhabditis elegans*. Oxid Med Cell Longev. 2019; 2019:5768953.
https://doi.org/10.1155/2019/5768953
PMID:31249646

37. Prasain JK, Wilson L, Hoang HD, Moore R, Miller MA. Comparative Lipidomics of Caenorhabditis elegans Metabolic Disease Models by SWATH Non-Targeted Tandem Mass Spectrometry. Metabolites. 2015; 5:677–96.
https://doi.org/10.3390/metabo5040677
PMID:26569325

38. Chan JP, Brown J, Hark B, Nolan A, Servello D, Hrobuchak H, Staab TA. Loss of Sphingosine Kinase Alters Life History Traits and Locomotor Function in *Caenorhabditis elegans*. Front Genet. 2017; 8:132.
https://doi.org/10.3389/fgene.2017.00132
PMID:28983319

39. Hannun YA, Obeid LM. Sphingolipids and their metabolism in physiology and disease. Nat Rev Mol Cell Biol. 2018; 19:175–91.
https://doi.org/10.1038/nrm.2017.107
PMID:29165427

40. Menuz V, Howell KS, Gentina S, Epstein S, Riezman I, Fornallaz-Mulhauser M, Hengartner MO, Gomez M, Riezman H, Martinou JC. Protection of C. elegans from anoxia by HYL-2 ceramide synthase. Science. 2009; 324:381–4.
https://doi.org/10.1126/science.1168532
PMID:19372430

41. O'Rourke EJ, Soukas AA, Carr CE, Ruvkun G. C. elegans major fats are stored in vesicles distinct from lysosome-related organelles. Cell Metab. 2009; 10:430–5.
https://doi.org/10.1016/j.cmet.2009.10.002
PMID:19883620

42. Escorcia W, Ruter DL, Nhan J, Curran SP. Quantification of Lipid Abundance and Evaluation of Lipid Distribution in Caenorhabditis elegans by Nile Red and Oil Red O Staining. J Vis Exp. 2018; 57352.
https://doi.org/10.3791/57352 PMID:29553519

43. Kubagawa HM, Watts JL, Corrigan C, Edmonds JW, Sztul E, Browse J, Miller MA. Oocyte signals derived from polyunsaturated fatty acids control sperm recruitment *in vivo.* Nat Cell Biol. 2006; 8:1143–8.
https://doi.org/10.1038/ncb1476
PMID:16998478

44. Christie WW. Preparation of lipid extracts from tissues. 1993.

45. Hänel V, Pendleton C, Witting M. The sphingolipidome of the model organism Caenorhabditis elegans. Chem Phys Lipids. 2019; 222:15–22.
https://doi.org/10.1016/j.chemphyslip.2019.04.009
PMID:31028715

46. Brooks KK, Liang B, Watts JL. The influence of bacterial diet on fat storage in C. elegans. PLoS One. 2009; 4:e7545.
https://doi.org/10.1371/journal.pone.0007545
PMID:19844570

47. Bar DZ, Charar C, Dorfman J, Yadid T, Tafforeau L, Lafontaine DL, Gruenbaum Y. Cell size and fat content of dietary-restricted Caenorhabditis elegans are regulated by ATX-2, an mTOR repressor. Proc Natl Acad Sci USA. 2016; 113:E4620–9.
https://doi.org/10.1073/pnas.1512156113
PMID:27457958

48. Law SH, Chan ML, Marathe GK, Parveen F, Chen CH, Ke LY. An Updated Review of Lysophosphatidylcholine Metabolism in Human Diseases. Int J Mol Sci. 2019; 20:1149.
https://doi.org/10.3390/ijms20051149
PMID:30845751

49. Engel KM, Schiller J, Galuska CE, Fuchs B. Phospholipases and Reactive Oxygen Species Derived Lipid Biomarkers in Healthy and Diseased Humans and Animals - A Focus on Lysophosphatidylcholine. Front Physiol. 2021; 12:732319.
https://doi.org/10.3389/fphys.2021.732319
PMID:34858200

50. Shmookler Reis RJ, Xu L, Lee H, Chae M, Thaden JJ, Bharill P, Tazearslan C, Siegel E, Alla R, Zimniak P, Ayyadevara S. Modulation of lipid biosynthesis

contributes to stress resistance and longevity of C. elegans mutants. Aging (Albany NY). 2011; 3:125–47.
https://doi.org/10.18632/aging.100275
PMID:21386131

51. Kniazeva M, Crawford QT, Seiber M, Wang CY, Han M. Monomethyl branched-chain fatty acids play an essential role in Caenorhabditis elegans development. PLoS Biol. 2004; 2:E257.
https://doi.org/10.1371/journal.pbio.0020257
PMID:15340492

52. Kniazeva M, Euler T, Han M. A branched-chain fatty acid is involved in post-embryonic growth control in parallel to the insulin receptor pathway and its biosynthesis is feedback-regulated in C. elegans. Genes Dev. 2008; 22:2102–10.
https://doi.org/10.1101/gad.1692008 PMID:18676815

53. Watts JL, Ristow M. Lipid and Carbohydrate Metabolism in *Caenorhabditis elegans*. Genetics. 2017; 207:413–46.
https://doi.org/10.1534/genetics.117.300106
PMID:28978773

54. Hannich JT, Mellal D, Feng S, Zumbuehl A, Riezman H. Structure and conserved function of iso-branched sphingoid bases from the nematode *Caenorhabditis elegans*. Chem Sci. 2017; 8:3676–86.
https://doi.org/10.1039/c6sc04831e PMID:30155209

55. Deng X, Kolesnick R. Caenorhabditis elegans as a model to study sphingolipid signaling. Biol Chem. 2015; 396:767–73.
https://doi.org/10.1515/hsz-2014-0298
PMID:25720116

56. Barbacini P, Torretta E, Arosio B, Ferri E, Capitanio D, Moriggi M, Gelfi C. Novel Insight into the Serum Sphingolipid Fingerprint Characterizing Longevity. Int J Mol Sci. 2022; 23:2428.
https://doi.org/10.3390/ijms23052428
PMID:35269570

57. Pradas I, Jové M, Huynh K, Ingles M, Borras C, Mota-Martorell N, Galo-Licona JD, Puig J, Viña J, Meikle PJ, Pamplona R. Long-lived Humans Have a Unique Plasma Sphingolipidome. J Gerontol A Biol Sci Med Sci. 2022; 77:728–35.
https://doi.org/10.1093/gerona/glab360
PMID:34871393

58. Chiantia S, London E. Acyl chain length and saturation modulate interleaflet coupling in asymmetric bilayers: effects on dynamics and structural order. Biophys J. 2012; 103:2311–9.
https://doi.org/10.1016/j.bpj.2012.10.033
PMID:23283230

59. Wahnon R, Mokady S, Cogan U. Age and membrane fluidity. Mech Ageing Dev. 1989; 50:249–55.

https://doi.org/10.1016/0047-6374(89)90103-6
PMID:2630834

60. Wi JH, Heo CH, Gwak H, Jung C, Kim SY. Probing Physical Properties of the Cellular Membrane in Senescent Cells by Fluorescence Imaging. J Phys Chem B. 2021; 125:10182–94.
https://doi.org/10.1021/acs.jpcb.1c05403
PMID:34473497

61. Jeśko H, Stępień A, Lukiw WJ, Strosznajder RP. The Cross-Talk Between Sphingolipids and Insulin-Like Growth Factor Signaling: Significance for Aging and Neurodegeneration. Mol Neurobiol. 2019; 56:3501–21.
https://doi.org/10.1007/s12035-018-1286-3
PMID:30140974

62. Hanamatsu H, Ohnishi S, Sakai S, Yuyama K, Mitsutake S, Takeda H, Hashino S, Igarashi Y. Altered levels of serum sphingomyelin and ceramide containing distinct acyl chains in young obese adults. Nutr Diabetes. 2014; 4:e141.
https://doi.org/10.1038/nutd.2014.38 PMID:25329603

63. Wang F, Dai Y, Zhu X, Chen Q, Zhu H, Zhou B, Tang H, Pang S. Saturated very long chain fatty acid configures glycosphingolipid for lysosome homeostasis in long-lived C. elegans. Nat Commun. 2021; 12:5073.
https://doi.org/10.1038/s41467-021-25398-6
PMID:34417467

64. Govindan JA, Jayamani E, Zhang X, Breen P, Larkins-Ford J, Mylonakis E, Ruvkun G. Lipid signalling couples translational surveillance to systemic detoxification in Caenorhabditis elegans. Nat Cell Biol. 2015; 17:1294–303.
https://doi.org/10.1038/ncb3229 PMID:26322678

65. Li Z, Zhang H, Liu J, Liang CP, Li Y, Li Y, Teitelman G, Beyer T, Bui HH, Peake DA, Zhang Y, Sanders PE, Kuo MS, et al. Reducing plasma membrane sphingomyelin increases insulin sensitivity. Mol Cell Biol. 2011; 31:4205–18.
https://doi.org/10.1128/MCB.05893-11
PMID:21844222

66. Chen X, Li J, Gao Z, Yang Y, Kuang W, Dong Y, Chua GH, Huang X, Jiang B, Tian H, Wang Y, Huang X, Li Y, et al. Endogenous ceramide phosphoethanolamine modulates circadian rhythm via neural-glial coupling in *Drosophila*. Natl Sci Rev. 2022; 9:nwac148.
https://doi.org/10.1093/nsr/nwac148
PMID:36713590

67. Darios F, Wasser C, Shakirzyanova A, Giniatullin A, Goodman K, Munoz-Bravo JL, Raingo J, Jorgacevski J, Kreft M, Zorec R, Rosa JM, Gandia L, Gutiérrez LM, et al. Sphingosine facilitates SNARE complex assembly and activates synaptic vesicle exocytosis. Neuron. 2009; 62:683–94.

https://doi.org/10.1016/j.neuron.2009.04.024
PMID:19524527

68. Nelson JC, Jiang XC, Tabas I, Tall A, Shea S. Plasma sphingomyelin and subclinical atherosclerosis: findings from the multi-ethnic study of atherosclerosis. Am J Epidemiol. 2006; 163:903–12.
https://doi.org/10.1093/aje/kwj140 PMID:16611667

69. Ackerman D, Gems D. The mystery of C. elegans aging: an emerging role for fat. Distant parallels between C. elegans aging and metabolic syndrome? Bioessays. 2012; 34:466–71.
https://doi.org/10.1002/bies.201100189
PMID:22371137

70. Shi X, Li J, Zou X, Greggain J, Rødkær SV, Færgeman NJ, Liang B, Watts JL. Regulation of lipid droplet size and phospholipid composition by stearoyl-CoA desaturase. J Lipid Res. 2013; 54:2504–14.
https://doi.org/10.1194/jlr.M039669 PMID:23787165

71. Vrablik TL, Petyuk VA, Larson EM, Smith RD, Watts JL. Lipidomic and proteomic analysis of Caenorhabditis elegans lipid droplets and identification of ACS-4 as a lipid droplet-associated protein. Biochim Biophys Acta. 2015; 1851:1337–45.
https://doi.org/10.1016/j.bbalip.2015.06.004
PMID:26121959

72. Berg M, Zhou XY, Shapira M. Host-Specific Functional Significance of *Caenorhabditis* Gut Commensals. Front Microbiol. 2016; 7:1622.
https://doi.org/10.3389/fmicb.2016.01622
PMID:27799924

73. Handee W, Li X, Hall KW, Deng X, Li P, Benning C, Williams BL, Kuo MH. An Energy-Independent Pro-longevity Function of Triacylglycerol in Yeast. PLoS Genet. 2016; 12:e1005878.
https://doi.org/10.1371/journal.pgen.1005878
PMID:26907989

74. Lapierre LR, Silvestrini MJ, Nuñez L, Ames K, Wong S, Le TT, Hansen M, Meléndez A. Autophagy genes are required for normal lipid levels in C. elegans. Autophagy. 2013; 9:278–86.
https://doi.org/10.4161/auto.22930 PMID:23321914

75. Yang P, Zhang H. You are what you eat: multifaceted functions of autophagy during C. elegans development. Cell Res. 2014; 24:80–91.
https://doi.org/10.1038/cr.2013.154
PMID:24296782

76. Lapierre LR, Gelino S, Meléndez A, Hansen M. Autophagy and lipid metabolism coordinately modulate life span in germline-less C. elegans. Curr Biol. 2011; 21:1507–14.
https://doi.org/10.1016/j.cub.2011.07.042
PMID:21906946

77. Jenkins RW, Canals D, Hannun YA. Roles and regulation of secretory and lysosomal acid sphingomyelinase. Cell Signal. 2009; 21:836–46.
https://doi.org/10.1016/j.cellsig.2009.01.026
PMID:19385042

78. Schmökel V, Memar N, Wiekenberg A, Trotzmüller M, Schnabel R, Döring F. Genetics of Lipid-Storage Management in Caenorhabditis elegans Embryos. Genetics. 2016; 202:1071–83.
https://doi.org/10.1534/genetics.115.179127
PMID:26773047

79. Wolff S, Dillin A. The trifecta of aging in Caenorhabditis elegans. Exp Gerontol. 2006; 41:894–903.
https://doi.org/10.1016/j.exger.2006.06.054
PMID:16919905

80. Liguori I, Russo G, Curcio F, Bulli G, Aran L, Della-Morte D, Gargiulo G, Testa G, Cacciatore F, Bonaduce D, Abete P. Oxidative stress, aging, and diseases. Clin Interv Aging. 2018; 13:757–72.
https://doi.org/10.2147/CIA.S158513 PMID:29731617

81. O'Rourke EJ, Kuballa P, Xavier R, Ruvkun G. ω-6 Polyunsaturated fatty acids extend life span through the activation of autophagy. Genes Dev. 2013; 27:429–40.
https://doi.org/10.1101/gad.205294.112
PMID:23392608

82. Rabini RA, Moretti N, Staffolani R, Salvolini E, Nanetti L, Franceschi C, Mazzanti L. Reduced susceptibility to peroxidation of erythrocyte plasma membranes from centenarians. Exp Gerontol. 2002; 37:657–63.
https://doi.org/10.1016/s0531-5565(02)00006-2
PMID:11909683

83. Depuydt G, Xie F, Petyuk VA, Smolders A, Brewer HM, Camp DG 2nd, Smith RD, Braeckman BP. LC-MS proteomics analysis of the insulin/IGF-1-deficient Caenorhabditis elegans daf-2(e1370) mutant reveals extensive restructuring of intermediary metabolism. J Proteome Res. 2014; 13:1938–56.
https://doi.org/10.1021/pr401081b PMID:24555535

84. Samuelson AV, Carr CE, Ruvkun G. Gene activities that mediate increased life span of C. elegans insulin-like signaling mutants. Genes Dev. 2007; 21:2976–94.
https://doi.org/10.1101/gad.1588907
PMID:18006689

85. Cheng X, Jiang X, Tam KY, Li G, Zheng J, Zhang H. Sphingolipidomic Analysis of *C. elegans* reveals Development- and Environment-dependent Metabolic Features. Int J Biol Sci. 2019; 15:2897–10.
https://doi.org/10.7150/ijbs.30499 PMID:31853226

86. Zou Y, Kim DH, Jung KJ, Heo HS, Kim CH, Baik HS, Yu BP, Yokozawa T, Chung HY. Lysophosphatidylcholine enhances oxidative stress via the 5-lipoxygenase

pathway in rat aorta during aging. Rejuvenation Res. 2009; 12:15–24.
https://doi.org/10.1089/rej.2008.0807
PMID:19226207

87. Burton NO, Dwivedi VK, Burkhart KB, Kaplan RE, Baugh LR, Horvitz HR. Neurohormonal signaling via a sulfotransferase antagonizes insulin-like signaling to regulate a Caenorhabditis elegans stress response. Nat Commun. 2018; 9:5152.
https://doi.org/10.1038/s41467-018-07640-w
PMID:30514845

88. Li P, Wang Z, Lam SM, Shui G. Rebaudioside A Enhances Resistance to Oxidative Stress and Extends Lifespan and Healthspan in *Caenorhabditis elegans*. Antioxidants (Basel). 2021; 10:262.
https://doi.org/10.3390/antiox10020262
PMID:33567712

89. Possik E, Pause A. Measuring oxidative stress resistance of Caenorhabditis elegans in 96-well microtiter plates. J Vis Exp. 2015; e52746.
https://doi.org/10.3791/52746 PMID:25993260

90. Schneider CA, Rasband WS, Eliceiri KW. NIH Image to ImageJ: 25 years of image analysis. Nat Methods. 2012; 9:671–75.
https://doi.org/10.1038/nmeth.2089
PMID:22930834

91. Hanson AJ, Banks WA, Bettcher LF, Pepin R, Raftery D, Craft S. Cerebrospinal fluid lipidomics: effects of an intravenous triglyceride infusion and apoE status. Metabolomics. 2019; 16:6.
https://doi.org/10.1007/s11306-019-1627-x
PMID:31832778

92. Ghorasaini M, Mohammed Y, Adamski J, Bettcher L, Bowden JA, Cabruja M, Contrepois K, Ellenberger M, Gajera B, Haid M, Hornburg D, Hunter C, Jones CM, et al. Cross-Laboratory Standardization of Preclinical Lipidomics Using Differential Mobility Spectrometry and Multiple Reaction Monitoring. Anal Chem. 2021; 93:16369–78.
https://doi.org/10.1021/acs.analchem.1c02826
PMID:34859676

93. Wei R, Wang J, Su M, Jia E, Chen S, Chen T, Ni Y. Missing Value Imputation Approach for Mass Spectrometry-based Metabolomics Data. Sci Rep. 2018; 8:663.
https://doi.org/10.1038/s41598-017-19120-0
PMID:29330539

94. Ritchie ME, Phipson B, Wu D, Hu Y, Law CW, Shi W, Smyth GK. limma powers differential expression analyses for RNA-sequencing and microarray studies. Nucleic Acids Res. 2015; 43:e47.
https://doi.org/10.1093/nar/gkv007
PMID:25605792

95. Smyth GK. Linear models and empirical bayes methods for assessing differential expression in microarray experiments. Stat Appl Genet Mol Biol. 2004; 3:Article3.
https://doi.org/10.2202/1544-6115.1027
PMID:16646809
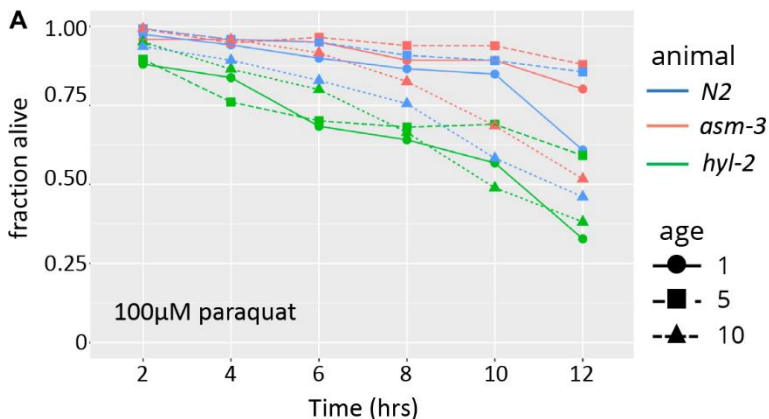
Supplementary Figure 1. *hyl-2*/ceramide synthase animals show poor response to paraquat. (**A**) Survival of 1-, 5-, and 10-day old N2 (blue), *asm-3* (red), and *hyl-2* (green) worms exposed to 100μM paraquat. Worms were treated with paraquat in 96 well plates, and response to agitation was recorded every two hours to determine survival. Each group was done in 6 replicates of 10 worms each.
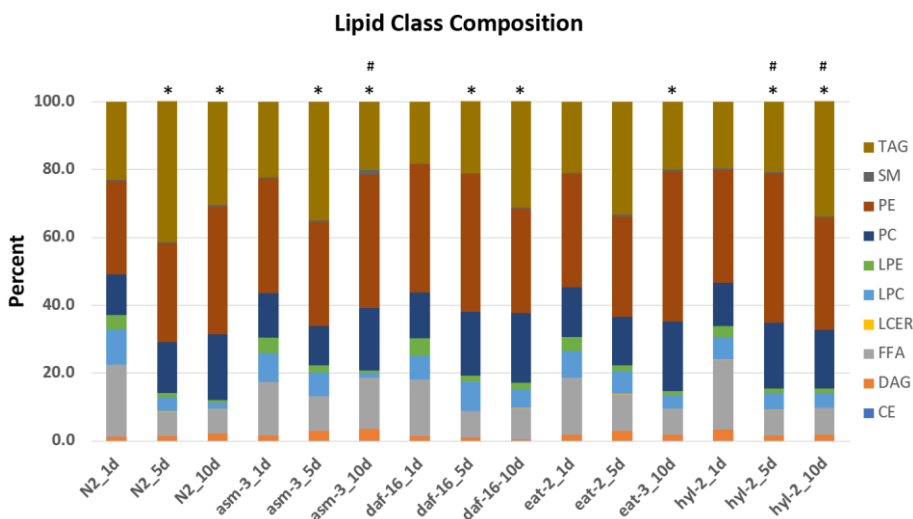
Supplementary Figure 2. Lipid class composition changes as animals age. The percentages were calculated as the proportion of the total lipids (nmol/g of worm tissue (μM)) in each class divided by total lipids in the group. The percentages were then compared to the 1-day N2 animals (* indicates $p<0.05$ compared to N2_1d). Each 5- and 10- day was also compared to the 1-day group for each strain (# indicates $p<0.05$ compared to 1d counterpart). Comparisons were performed using Chi Sq analyses.

Sphingomyelins (SMs) in 1, 5, and 10-day old N2, *asm-3*, and *hyl-2* animals
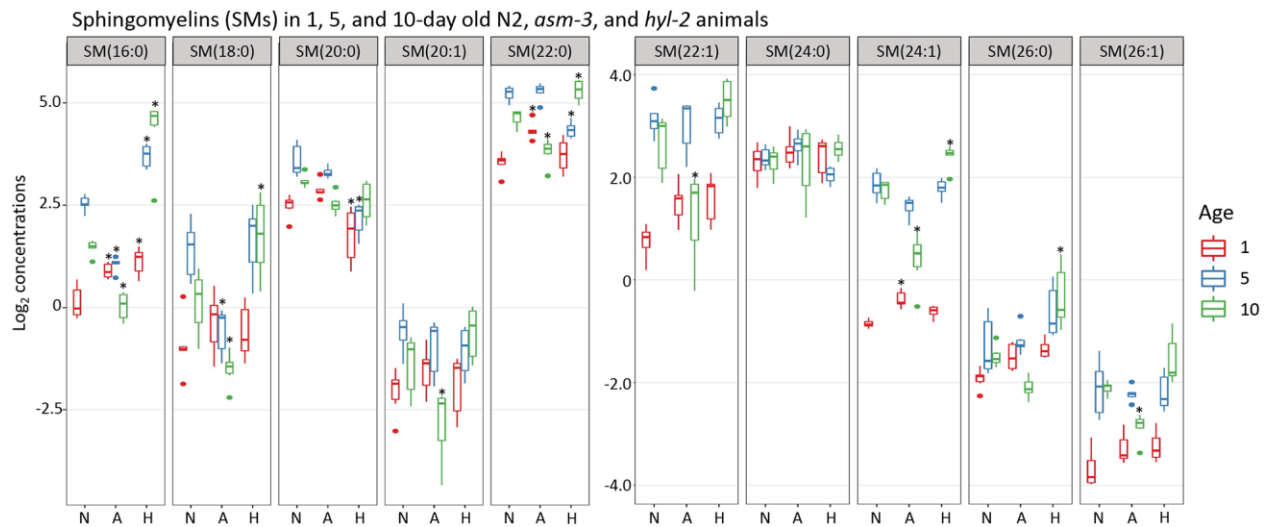
Supplementary Figure 3. Sphingomyelin changes by age in sphingolipid mutants. The boxplots show log2 concentrations of respective sphingolipids in N2 (N), *asm-3*/acid sphingomyelinase (A) and *hyl-2*/ceramide synthase (H) animals. For sphingomyelins, the lipid ID does not include the 18:1 fatty acid chain, and LIPIDMAPS nomenclature is reported in Supplementary table 11. For all, n=6 and * indicates $p<0.05$ compared only to N2 animals of the same age (ANOVA and Tukey-HSD tests).

TAG containing FA15:0 or FA:17
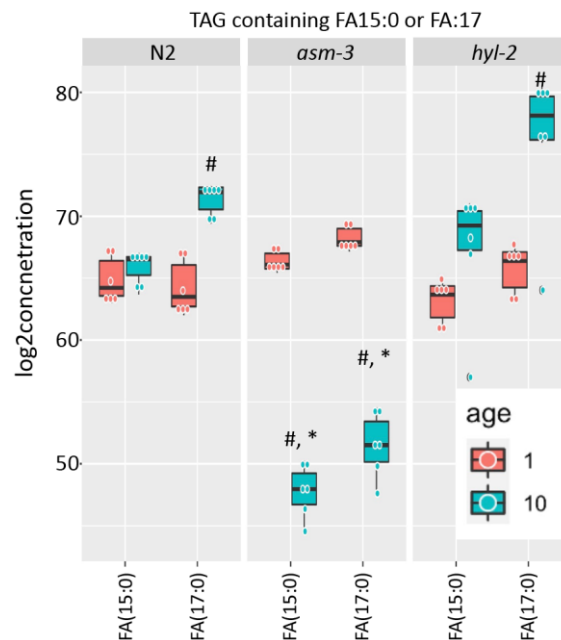
Supplementary Figure 4. Triacylglyercols containing FA15:0 and FA17:0 are increased in asm-3/acid sphingomyelinase mutants. Total Log_2 concentrations of TAG containing FA(15:0) and FA(17:0) chains were summed for 1- and 10-day old N2, *asm-3*, and *hyl-2* animals (n=6 for each group). When comparing N2 and asm-3, there was a significant difference between TAGs containing FA15:0 and FA17:0, and pairwise analyses show significant differences between 10-day concentrations ($p<0.000001$ for FA15:0 and $p<0.000001$ for FA17:0) but not 1-day concentrations. For comparisons between N2 and hyl-2, there was also a significant difference between N2 and hyl-2 animals, but pairwise analysis did not show significant differences between 10-day concentrations ($p=0.93$ for FA15:0 and $p=0.11$ for FA17:0). For all, #indicates $p<0.05$ compared to 1-day counterpart of the same genotype. *indicates $p<0.05$ compared to N2 counterpart of the same age.

Supplementary Tables

Please browse Full Text version to see the data of Supplementary Tables 2, 3, 4, 5, 7, 8, 9.

Supplemental Table 1. Primer sequences for genes used in qPCR.

Gene	Primer sequence (3' - 5')
elo-1	
Forward	CAGTTGGCATTGGTGAAGTGC
Reverse	CCAGGATTCAACAGATACGGA
elo-2	
Forward	GGGTTTGTCGCTTCCTACTG
Reverse	TCAGAGTATGTGACTACTGCG
elo-5	
Forward	ATGCACTGGTACCATCACGC
Reverse	ATGGCAACTGCGAATTGAACC
elo-6	
Forward	AACCATTTGATCTCACGGGACC
Reverse	CACGGCTGAAGAACTCGTGG
fat-1	
Forward	CTTCACCATGCTTTCACCAACC
Reverse	CCGAATAAAGTGTACACTGGG
fat-4	
Forward	GGAGAAGTTTGCATTGAGCTCG
Reverse	TGTGTCGTGGCATCGTTGG
fat-6	
Forward	TCTGATCTCTTGAGTGACCC
Reverse	ATCCGAAATAGTGAGCAGCG
fat-7	
Forward	ACGGCCGTCTTCTCATTTGCT
Reverse	TGGCAACGATGATCACGAGC
cup-16	
Forward	TCGAAGAGAGCACTTAACGGC
Reverse	GCAGATGTTTCAGCGCCTATT
rpl-2	
Forward	TGTGGAGCTAAGGCTCAAATC
Reverse	CGTTGCAGATGGTGGTTCCTT
hyl-2	
Forward	GACCAGAAGGGGAACACTGG
Reverse	CGAGAGCAATGTAGAATCCTCC
sptl-1	
Forward	GAAGAGGAGTCACCGAGCA
Reverse	CCGTTGCAAGAAGAGGTGG
sphk-1	
Forward	ATTCGCAGCTGCAATCTCCG
Reverse	GAATCTGACACGGATCCATTCG
rpl-2	
Forward	TGTGGAGCTAAGGCTCAAATC
Reverse	CGTTGCAGATGGTGGTTCCTT
fat-2	
Forward	GGATATTGAGGTCTACGAAGC
Rreverse	AAGTGATGGGCGACGTGAC

Supplemental Table 2. Lipid fold changes between wild type (N2) 10-day and 1-day old animals.

Supplemental Table 3. Lipid fold changes between 10-day N2 and 10-day asm-3 animals.

Supplemental Table 4. Lipid fold changes between 10-day N2 and 10-day hyl-2 animals.

Supplemental Table 5. Lipid fold changes between 5-day N2 and 1-day N2 animals.

Supplemental Table 6. Lipid fold changes between 10-day N2 and 10-day eat-2 animals.

Lipid	LogFC	P.Value	FDR
TAG44:1-FA14:1	-5.05071	3.27E-22	1.15E-19
TAG46:3-FA14:0	-3.11684	0.00000000000068	0.0000000000144
TAG45:0-FA15:0	-2.75904	2.37E-24	1.66E-21
TAG46:2-FA18:2	-2.73781	0.000000000000293	0.00000000000684
TAG44:0-FA12:0	-2.72853	0.00000000717	0.0000000529
TAG50:2-FA20:2	-2.67452	1.62E-20	2.84E-18
TAG46:0-FA18:0	-2.66131	0.0000000038	0.0000000296
TAG42:0-FA14:0	-2.65593	0.000276	0.000759
TAG48:4-FA14:1	-2.5399	0.0000000000000000196	0.00000000000000132
TAG50:4-FA14:1	-2.51176	1.06E-18	0.000000000000000932
TAG46:1-FA14:1	-2.50983	1.31E-19	0.000000000000000173
TAG46:0-FA12:0	-2.46487	0.00000682	0.000027
TAG52:2-FA20:2	-2.3372	7.3E-19	0.0000000000000000731
TAG44:3-FA18:2	-2.3253	0.000000872	0.00000413
TAG48:3-FA18:3	-2.3128	0.00000000000125	0.0000000000237
TAG47:0-FA15:0	-2.29485	1.48E-19	0.000000000000000173
TAG48:2-FA18:2	-2.2154	0.0000000000000000539	0.0000000000000027
TAG46:2-FA14:1	-2.2092	0.0000000000000000208	0.00000000000000132
TAG44:1-FA18:1	-2.19892	0.00000000000134	0.0000000000247
TAG50:1-FA20:1	-2.19501	0.0000000000000000525	0.0000000000000027
TAG46:3-FA18:2	-2.18545	0.0000000000000115	0.000000000000424
TAG50:5-FA18:2	-2.16965	0.0000000114	0.0000000813
TAG47:0-FA17:0	-2.16637	6.85E-18	0.000000000000000534
TAG45:1-FA15:0	-2.15197	0.000000000000000234	0.000000000000011
TAG42:1-FA14:0	-2.10766	0.0000854	0.000259
TAG48:1-FA14:1	-2.09764	0.0000000000000000525	0.0000000000000027
TAG46:1-FA16:1	-2.08682	0.000000000000133	0.000000000000465
TAG47:2-FA18:2	-2.05378	0.0000000000000278	0.000000000000122
LPE(20:4)	2.002917	0.00000000413	0.0000000318
CE(20:4)	2.058696	0.00000147	0.00000647
PE(18:1/18:4)	2.116137	0.00000333	0.000014
LPC(20:0)	2.15351	0.003403	0.007454
PE(18:0/18:4)	2.728121	0.00000000124	0.0000000108

Supplemental Table 7. Lipid changes between 10-day N2 and 10-day daf-16 animals.

Supplemental Table 8. Comparative lipid changes between 10- and 1-day asm-3 animals vs 10- and 1-day N2 animals.

Supplemental Table 9. Comparative lipid changes between 10- and 1-day hyl2 animals ve 10- and 1-day N2 animals.

Supplemental Table 10. Relative gene expression and fold change values from RT-qPCR analyses of 10-day and 1-day WT, asm-3 and hyl-2 animals.

		1day			10day			10day/1day		
Gene	Animal	2ddCT	SEofdiff	p value (vs N2)	2ddCT	SE	p value (vs N2)	FC	log2FC	p value
rpl-2	N2	1	0.37	n/a	1.12	0.35	n/a	1.32	0.17	0.998
rpl-2	hyl-2	1.21	0.28	0.984	1.28	0.38	0.997	1.03	0.08	1
rpl-2	asm-3	0.94	0.4	1	1.56	0.69	0.865	1.74	0.73	0.542
elo-5	N2	1	0.75	n/a	0.24	0.5	n/a	-4.13	-2.05	0.005
elo-5	hyl-2	2.05	0.54	0.902	0.42	0.33	0.149	-4.92	-2.3	0.002
elo-5	asm-3	1.22	0.61	0.232	0.54	0.75	0.496	-2.25	-1.17	0.144
elo-6	N2	1	0.7	n/a	0.39	0.51	n/a	-2.57	-1.36	0.081
elo-6	hyl-2	1.74	0.48	0.501	0.34	0.51	0.997	-5.13	-2.36	0.002
elo-6	asm-3	1.41	0.41	0.867	0.7	0.64	0.44	-2.01	-1.01	0.276
elo-1	N2	1	0.33	n/a	0.96	0.65	n/a	-1.04	-0.06	1
elo-1	hyl-2	0.71	0.27	0.696	1.23	0.63	0.881	1.73	0.79	0.245
elo-1	asm-3	1.14	0.48	0.993	1.47	0.72	0.488	1.29	0.37	0.873
elo-2	N2	1	0.35	n/a	0.44	0.63	n/a	-2.27	-1.18	0.161
elo-2	hyl-2	0.45	0.39	0.182	1.01	1	0.15	2.24	1.16	0.17
elo-2	asm-3	2	0.49	0.293	1.03	0.72	0.142	-1.95	-0.96	0.327
fat-1	N2	1	0.37	n/a	1.12	0.35	n/a	1.12	0.17	0.923
fat-1	hyl-2	1.21	0.28	0.753	1.28	0.38	0.995	1.06	0.08	0.43
fat-1	asm-3	0.94	0.4	0.998	1.56	0.69	0.735	1.66	0.73	1
fat-2	N2	1	0.67	n/a	0.63	0.71	n/a	0.63	-0.67	1
fat-2	hyl-2	1.18	0.67	0.683	0.86	0.71	0.865	0.73	-0.46	0.998
fat-2	asm-3	0.69	0.58	0.998	1.25	0.64	0.361	1.81	0.86	0.667
fat-4	N2	1	0.41	n/a	0.81	0.48	n/a	-1.23	-0.3	0.936
fat-4	hyl-2	1.29	0.49	0.863	0.91	0.5	0.996	-1.43	-0.51	0.637
fat-4	asm-3	0.8	0.45	0.803	1.72	0.66	0.056	2.16	1.11	0.049
fat-6	N2	1	0.7	n/a	0.44	0.66	n/a	0.44	-1.18	0.669
fat-6	hyl-2	1.37	0.75	0.83	0.87	0.91	0.316	0.64	-0.66	0.993
fat-6	asm-3	0.8	0.77	1	1	0.93	0.616	1.25	0.32	1
fat-7	N2	1	0.69	n/a	0.04	0.63	n/a	0.04	-4.64	0
fat-7	hyl-2	0.81	0.69	0.968	0.01	0.79	0	0.01	-6.34	0
fat-7	asm-3	0.46	0.72	0.516	0.03	0.8	0.201	0.07	-3.94	0
asm-3	N2	1	0.69	n/a	0.2	1.1	n/a	-4.91	-2.3	0.226
asm-3	hyl-2	2.33	0.72	0.762	0.07	1.2	0.666	-33.51	-5.07	0.01
asm-3	asm-3			n/a			n/a			
hyl-2	N2	1	0.77	n/a	3	0.93	n/a	3	1.58	0.241
hyl-2	hyl-2			n/a			n/a			
hyl-2	asm-3	1.29	0.66	0.992	4.13	0.84	0.979	3.2	1.68	0.196
cup-16	N2	1	0.4	n/a	11.26	0.87	n/a	11.26	3.49	0
cup-16	hyl-2	0.76	0.59	0.949	17.35	0.77	0.764	22.94	4.52	0
cup-16	asm-3	0.81	0.53	0.984	22.01	0.79	0.366	27.22	4.77	0
sptl-1	N2	1	0.94	n/a	1.17	1.13	n/a	1.17	0.23	1
sptl-1	hyl-2	1.42	0.93	0.987	0.99	1.04	1	0.7	-0.52	0.985
sptl-1	asm-3	1.46	0.62	0.982	2.51	0.9	0.747	1.73	0.79	0.919
sphk-1	N2	1	0.59	n/a	1.08	0.8	n/a	1.077	0.11	1
sphk-1	hyl-2	1.09	0.78	1	1.57	0.9	0.919	1.441	0.53	0.928
sphk-1	asm-3	1.11	0.64	1	3.25	0.79	0.116	2.915	1.54	0.133

Supplementary Table 11. LIPIDMAPS and common names of sphingolipids examined.

	ID	HMDB	LIPIDMAPS	Common name
1	SM(14:0)	HMDB12097	LMSP03010028	SM(d18:1/14:0)
2	SM(16:0)	HMDB10169	LMSP03010003	SM(d18:1/16:0)
3	SM(18:0)	HMDB01348	LMSP03010001	SM(d18:1/18:0)
4	SM(18:1)	HMDB12101	LMSP03010029	SM(d18:1/18:1(9Z))
5	SM(20:0)	HMDB12102	LMSP03010005	SM(d18:1/20:0)
6	SM(20:1)	-	LMSP03010059	SM(d18:1/20:1)
7	SM(22:0)	HMDB12103	LMSP03010006	SM(d18:1/22:0)
8	SM(22:1)	HMDB12104	LMSP03010072	SM(d18:1/22:1)
9	SM(24:0)	HMDB11697	LMSP03010008	SM(d18:1/24:0)
10	SM(24:1)	HMDB12107	LMSP03010007	SM(d18:1/24:1(15Z))
11	SM(26:0)	HMDB11698	LMSP03010010	SM(d18:1/26:0)
12	SM(26:1)	-	LMSP03010009	SM(d18:1/26:1(17Z))